

MCH regulates SIRT1/FoxO1 and reduces POMC neuronal activity to induce hyperphagia, adiposity and glucose intolerance

Omar Al-Massadi^{1,2,*}, Mar Quiñones^{1,2,7,*}, Jerome Clasadonte^{3,10,*}, René H. Bautista¹, [Amparo Romero-Picó^{1,2}](#), [Cintia Folgueira^{1,2}](#), Donald A. Morgan⁴, Imre Kalló⁵, [Violeta Heras^{1,2}](#), [Ana Senra¹](#), Samuel C. Funderburk⁶, Michael J. Krashes⁶, Yara Souto¹, Miguel Fidalgo¹, Serge Luquet⁷, Melissa J Chee⁸, Monica Imbernon^{1,2,3}, Daniel Beiroa^{1,2}, Lucía García-Caballero⁹, Rosalia Gallego⁹, Brian Y. H. Lam¹¹, Giles Yeo¹¹, Miguel Lopez^{1,2}, Zsolt Liposits⁵, Kamal Rahmouni⁴, Vincent Prevot^{3,10}, Carlos Dieguez^{1,2}, Ruben Nogueiras^{1,2}

¹ Department of Physiology, CIMUS, University of Santiago de Compostela-Instituto de Investigación Sanitaria, Santiago de Compostela, 15782, Spain

² CIBER Fisiopatología de la Obesidad y Nutrición (CIBERObn), 15706, Spain

³ Inserm, Laboratory of Development and Plasticity of the Neuroendocrine Brain, Jean-Pierre Aubert Research Center, U1172, Lille, France

⁴ Department of Pharmacology, University of Iowa Carver College of Medicine and Veterans Affairs Health Care System, Iowa City, Iowa; USA

⁵ Laboratory of Endocrine Neurobiology, Institute of Experimental Medicine, Hungarian Academy of Sciences, Budapest, Hungary

⁶ Diabetes, Endocrinology and Obesity Branch, National Institutes of Diabetes and Digestive and Kidney Diseases, National Institutes of Health, Bethesda, Maryland 20892, USA.

⁷ Univ Paris Diderot, Sorbonne Paris Cité, Unité de Biologie Fonctionnelle et Adaptative, CNRS UMR 8251, F-75205 Paris, France.

⁸ Division of Endocrinology, Beth Israel Deaconess Medical Center, Department of Medicine, Harvard Medical School, Boston, MA 02215-5491, USA

⁹ Department of Morphological Sciences, School of Medicine, University of Santiago de Compostela-Instituto de Investigación Sanitaria, Santiago de Compostela, 15782, Spain

¹⁰ University of Lille, FHU 1000 days for Health, School of Medicine, Lille, France.

¹¹ MRC Metabolic Diseases Unit, University of Cambridge Metabolic Research Laboratories, Wellcome Trust-MRC Institute of Metabolic Science, Addenbrooke's Hospital, Cambridge, CB2 0QQ UK

* These authors contributed equally to this work

Short running title: [MCH inhibits POMC activity and requires SIRT1/FoxO1](#)

Correspondence (Lead Contact): Carlos Dieguez and Ruben Nogueiras, Department of Physiology, Centro de Investigaciones Médicas de la Universidad de Santiago (CIMUS), University of Santiago de Compostela & CIBER Fisiopatología de la Obesidad y Nutrición (CIBERObn); Avenida de Barcelona s/n, 15782 Santiago de Compostela (A Coruña), Spain. Emails: carlos.dieguez@usc.es or ruben.nogueiras@usc.es.

Abstract

Melanin concentrating hormone (MCH) is an important regulator of food intake, glucose metabolism and adiposity. However, the mechanisms mediating these actions remain largely unknown. We used pharmacological and genetic approaches to show that the SIRT1/FoxO1 signaling pathway in the hypothalamic arcuate nucleus (ARC) mediates MCH-induced feeding, adiposity and glucose intolerance. MCH reduces POMC neuronal activity and the SIRT1/FoxO1 pathway regulates the inhibitory effect of MCH on POMC expression. Remarkably, the metabolic actions of MCH are compromised in mice lacking SIRT1 specifically in POMC neurons. Of note, the actions of MCH are independent of AgRP neurons because inhibition of GABA-R in the ARC did not prevent the orexigenic action of MCH; and the hypophagic effect of MCH silencing was maintained after chemogenetic stimulation of AgRP neurons. Central SIRT1 is required for MCH-induced weight gain through its actions on the sympathetic nervous system. The central MCH knockdown causes hypophagia and weight loss in diet-induced obese wild type mice, however, these effects were abolished in mice over-expressing SIRT1 fed a high fat diet. These data reveal the neuronal basis for the effects of MCH on food intake, body weight and glucose metabolism and highlight the relevance of SIRT1/FoxO1 pathway in obesity.

Abbreviations

MCH: Melanin concentrating hormone; **MCHR1:** MCH receptor; **LHA:** lateral hypothalamic area; **SIRT1:** sirtuin 1; **POMC:** pro-opiomelanocortin; **AgRP:** Agouti related peptide; **FoxO1:** forkhead box O1; **ARC:** hypothalamic arcuate nucleus; **α MSH:** alpha melanocyte stimulating hormone; **MC3R:** melanocortin receptor 3; **MC4R:** melanocortin receptor 4; **DIO:** diet-induced obesity; **WAT:** white adipose tissue; **GLP-1:** glucagon-like peptide 1; **SNS:** sympathetic nervous system; **PSNS:** parasympathetic nervous system; **CART:** cocaine- and amphetamine-regulated transcript; **TG:** triglycerides; **AMPK:** AMP-activated protein kinase; **ACC:** acetyl-CoA carboxylase; **FAS:** fatty acid synthase.

Introduction

MCH is a 19-amino acid neuropeptide predominantly expressed in the LHA that plays a pivotal role in the regulation of energy homeostasis (1; 2). The central infusion of MCH induces feeding (3) and over-expression of MCH in transgenic mice leads to obesity (4). Conversely, pharmacological inhibition of MCHR1 reduces appetite, body weight and adiposity (5-7). In line with this, the lack of MCH causes hypophagia and leanness (8), attenuates leptin deficiency-induced obesity (9; 10), diet-induced obesity (DIO) (11), aging-associated increases in body weight and insulin resistance (12) and protects from hepatosteatosis (13). Independent of its actions on feeding and body weight, MCH induces insulin resistance (4; 14), and MCH-expressing neurons are stimulated by glucose and involved in the control of peripheral glucose homeostasis (15). In addition, MCH neurons are both necessary and sufficient for sensing the nutrient value of sucrose indicating that these neurons play a critical role in establishing nutrient preference (16). MCH also favors lipid storage in white adipose tissue (WAT) and liver through the sympathetic nervous system (SNS) and parasympathetic nervous system (PSNS), respectively (17).

MCH binds to MCHR1 (18), and MCHR1 deficient mice are lean, hypophagic and resistant to diet-induced obesity (19; 20). MCHR1 and MCH projections are widely distributed throughout the brain (21-26) suggesting that MCH is implicated in a large variety of functions. The complexity of the MCH system raises the possibility that multiple mechanisms underlie the biological actions of this neuropeptide. In line with this, MCH-induced food intake is blocked by different anorexigenic factors such as α -MSH (27; 28) , GLP-1 (28) and neuropeptide Y antagonism (29).

On the other hand, SIRT1 is a highly conserved NAD⁺-dependent deacetylase, which is activated in response to calorie restriction and acts as a cellular sensor to detect energy availability and regulate metabolism in a wide variety of tissues [for review see (30-32)]. Hypothalamic SIRT1 controls energy balance (33; 34) and these actions are at least partially mediated by the melanocortin system (35; 36). The lack of SIRT1 in POMC neurons leads to increased weight gain (37), while its deficiency in AgRP neurons leads to a lean phenotype (36).

Although the anabolic action of MCH was first shown nearly twenty years ago (3) and its physiological relevance is beyond any doubt, the neuronal circuits controlling this action remain largely unknown. We describe that MCH requires a SIRT1/FoxO1/POMC signaling pathway within the ARC to modulate feeding, adipocyte lipid metabolism and glucose metabolism.

Research design and methods

Animals and surgery

Eight-ten-week-old Sprague Dawley male rats, male C57/BL6 wild type (WT) and mice with moderate overexpression of SIRT1 (SIRT1 Tg) under the control of its own promoter, and Pomc-Cre:ROSA-tdTomato mice were housed in individual cages under conditions of controlled temperature (23°C) and illumination (12-hour light/12-hour dark cycle). Animals were allowed *ad libitum* access to water and standard laboratory chow or high fat diet (60% by energy, D12492, Research Diets, NJ, US). All experiments and procedures involved in this study were reviewed and approved by the Ethics Committee of the USC, the Institutional Ethics Committees for the Care and Use of Experimental Animals of the Universities of Lille and the University of Iowa Animal

Research Committee in accordance with EU normative for the use of experimental animals.

Patch-clamp recordings

Whole-cell patch-clamp recordings were performed in current-clamp mode as previously described (38) (see Supplemental information).

Intracerebroventricular infusions

ICV infusions in both rats and mice were conducted as described (39) (see Supplemental information).

Stereotaxic microinjection of lentiviral expression vectors

Lentiviral vectors expressing green fluorescent protein (GFP) and inhibiting SIRT1 (shSIRT1), FoxO1 (shFoxO1), MCHR1 (shMCHR1), POMC (shPOMC) ($3,1 \times 10^6$ PFU/ml) (SIGMA-Aldrich) and GABA-R (shGABA-R) genes or scrambled sequences were injected bilaterally into the ARC (anterior to bregma (AP) -2.85 mm, lateral to the sagittal suture (L) $\pm 0,3$ mm, and ventral from the surface of the skull (V) $-10,2$ mm), with a microliter syringe (17; 40-42). The viral particles ($1 \mu\text{l}$, $3,1 \times 10^6$ PFU/ml) were infused over 5 minutes and the injector kept in place for an additional 5 minutes. GFP fluorescence, visualized under the microscope, was used as a marker of effective transduction of the lentivirus at the injection site. Dissection of the ARC was performed by micropunches under the microscope, as previously reported (43; 44). The specificity of the ARC dissection was confirmed by analysing the mRNA of specific markers,

namely POMC and AgRP which expression was 80% higher in the ARC compared to VMH. To inhibit the expression of SIRT1 specifically in POMC neurons, we injected into the ARC AAV8-hSyn-DIO-GFP or AAV8-hSyn-shSIRT1-DIO-GFP of mice expressing Cre I POMC neurons. POMC-IRES-Cre, mice were anesthetized and placed in a stereotaxic frame (Kopf Instruments). Specific infection of AAV in POMC neurons was evaluated by immunohistochemistry. In all experimental settings body weight and food intake were recorded until 2-3 weeks after the surgery, and then, we perform the acute or chronic MCH treatments.

Western blot analysis and Real time PCR

Western blot and Real Time PCR were performed as described previously (17) (see Supplemental information).

Statistical analysis and data presentation

Data are expressed as mean \pm SEM. Protein data were expressed in relation (%) to control (vehicle or GFP-treated) rats/mice. SNA was expressed as a percent change from baseline. Statistical significance was determined by t-Student when two groups were compared or One-Way ANOVA and post hoc one-tailed Bonferroni test when more than two groups were compared. A $p < 0.05$ was considered significant.

Data and Resource Availability

The data that support the findings of this study are available from the corresponding author upon request.

Results

Central MCH stimulates FoxO1 and inhibits POMC protein levels via MCH-R in the ARC

As expected, an acute icv bolus of MCH increased feeding after 2h of injection in satiated Sprague Dawley rats (Figure 1A). Icv MCH-treated rats showed unchanged levels of hypothalamic pAMPK, p-mTOR and enzymes involved in fatty acid metabolism ([Supplementary Figure 1A](#)). However, MCH diminished acetyl-p53 levels, a surrogate marker of SIRT1 activity, and therefore decreased acetyl-FoxO1 levels, while raising FoxO1 protein levels in the hypothalamus (Figure 1B). Additionally, we found that central MCH significantly decreased POMC protein levels whereas no changes were observed in NPY, AgRP or CART (Figure 1C [and Supplementary Figure 1B](#)). Remarkably these molecular changes induced by MCH are observed also at the mRNA level ([Supplementary Figures 2A-2C](#)). Moreover, our results show the specificity of MCH-induced changes in FoxO1 and SIRT1 protein levels in the ARC, because those effects were not found in other hypothalamic areas such as the VMH or the lateral hypothalamic area ([Supplementary Figures 2D-2G](#)). Of note, the specificity of the isolation of hypothalamic nuclei was corroborated by measuring POMC and SF1 in the ARC and in the VMH ([Supplementary Figures 2H-2I](#)).

We combined ARC microinjection of vehicle or MCH with fluorescein-isothio-cyanate (FITC) that allowed us to control the diffusion of the treatment within the hypothalamus (Figure 1D). Consistent with bulk brain delivery of MCH, explicit targeting of MCH to the ARC stimulated food intake after 2h (Figure 1E), decreased acetyl-p53, acetyl-FoxO1 and POMC while increasing FoxO1 protein levels within the ARC (Figure 1F).

To elucidate the specific contribution of ARC MCHR1 to the hyperphagic effect of MCH, we used lentivirus encoding a shRNA that silence MCHR1. Two weeks later, infection efficiency was assessed by the expression of GFP in the ARC (Figure 1G) and by the decreased protein levels of MCHR1 in the ARC (Figure 1H). Inhibition of ARC MCHR1 blunted the orexigenic effect of icv MCH (Figure 1I), and blocked MCH effects on FoxO1 and POMC protein levels in the ARC (Figure 1J). These results indicate that MCH requires the MCHR1 in the ARC to induce feeding and to regulate FoxO1 and POMC in this hypothalamic nucleus.

MCH reduces the activity of POMC neurons

By using FACS sorting and single-cell RNA sequencing of 163 POMC eGFP neurons, we found that 19% of POMC neurons express MCH receptor (MCH-R1), 45% of POMC neurons express SIRT1 and 84% of POMC neurons express FoxO1 (GEO Database repository: GEO Accession: GSE92707) (Figure 2A). Since electrical activity of ARC POMC neurons changes across the hunger-satiety cycle and selective sustained opto- or chemogenetic stimulation of these cells promote satiety (45), we performed whole-cell current-clamp recordings from fluorescent labeled cells in acute brain slices from *Pomc-Cre:ROSA-tdTomato* mice (Figure 2B) to ask whether MCH-induced hyperphagia is also paralleled by decreased electrical activity of anorexigenic ARC POMC neurons. We found that bath application of 1 μ M MCH (46) reversibly reduced the spontaneous firing rate of 50% of ARC POMC neurons (6 out of 12 cells from 4 mice) by $58.92 \pm 11.39\%$ ($n=6$ cells from 4 mice) (Figures 2C and 2D), an effect that was accompanied by a membrane hyperpolarization of 6.83 ± 0.65 mV ($n=6$ cells from 4 mice) (Figures 2C and 2D). MCH had no effect on the 6 other cells tested (data not shown). Furthermore, the MCH-induced inhibitory effect on POMC neuronal firing

persisted in loose patch-clamp configuration (in 2 of 2 cells from 2 mice) (Figure 2E and 2F), indicating that it was not a consequence of dilution of the intracellular compartment by whole-cell dialysis. These results show that MCH inhibits the activity of ARC POMC neurons, an effect which together with the aforementioned MCH-induced downregulation of POMC gene expression in the ARC converge towards an inhibition of the anorexigenic POMC signaling.

Central MCH requires POMC but not AgRP to stimulate feeding

Since MCH decreases POMC levels and POMC activity, we hypothesized that MCH-antisense oligonucleotides (ASO), which are known to suppress feeding and to decrease MCH protein levels (data not shown), might require an up-regulation of POMC to exert their anorexigenic action. Thus, we next injected into the ARC a lentivirus encoding shRNA to silence POMC (Figure 3A) previous to the icv administration of MCH-ASO and found that the hypophagic action of MCH-ASO was blunted (Figure 3B). To rule out the potential role of AgRP neurons in the actions of MCH, we performed two additional studies. First, since AgRP neurons modulate POMC activity through the release of GABA, we silenced GABA-R in the ARC of rats [to test the possible regulation of AgRP neurons over POMC neuronal activity](#) (Figure 3C). The knockdown of ARC GABA-R did not alter MCH-induced hyperphagia (Figure 3D). Second, using DREADDs technology, we stimulated AgRP neurons in mice and found a clear stimulation of feeding, but the chemogenetic stimulation of AgRP neurons did not prevent the hypophagic action of the MCH-ASO (Figures 3E-3F). Thus, POMC but not AgRP is required for the orexigenic action of MCH.

Central MCH requires the interaction between SIRT1 and FoxO1 to stimulate feeding

We next assessed whether pharmacological or genetic blockade of SIRT1 interfere with the orexigenic action of MCH. Icv Ex527, a selective SIRT1 inhibitor, administered 20 min before icv MCH blunted the orexigenic action of MCH ([Supplementary Figure 3A](#)). Genetically inhibiting SIRT1 expression in the ARC via a lentivirus encoding a shRNA that silences SIRT1 (Figure 4A) blunted the orexigenic effect of icv MCH (Figure 4B), and blocked MCH-induced changes in FoxO1 and POMC protein levels in the ARC (Figure 4C). Of note, the titer and volume of lentiviruses encoding shSIRT1 used for these manipulations did not cause alterations in physiological body weight or food intake ([Supplementary Figures 3B-3C](#)). To evaluate the role of FoxO1 as the downstream mediator of SIRT1-dependent MCH orexigenic action, we administered into the ARC a lentivirus encoding a shRNA that silence FoxO1 (Figure 4D). Inhibition of ARC FoxO1 partially blocked the orexigenic effect of icv MCH (Figure 4E) and reversed the effects of MCH on POMC protein levels in the ARC (Figure 4F).

ARC SIRT1 and FoxO1 are necessary for central MCH to promote adipocyte lipid storage and glucose intolerance

In order to study the role of SIRT1/FoxO1 pathway in central actions of MCH on adipocyte metabolism and glucose metabolism, we administered into the ARC a lentivirus encoding a shRNA SIRT1 together with GFP or adenovirus expressing GFP scrambled shRNA (control). Two weeks later, rats in each group received icv MCH or vehicle (saline) [for](#) one week. While chronic central infusion of MCH significantly induced weight gain and food intake, these effects were abolished in rats in which SIRT1 was silenced in the ARC (Figures 5A and 5B). Consistent with the increased

weight gain and previous report (17), MCH decreased WAT protein levels of pHSL and pJNK and increased CIDEA (Figure 5C). ARC SIRT1 silencing abolished these effects evoked by MCH in WAT (Figure 5C). In order to test if the actions of central MCH on WAT were mediated by thermogenesis or browning of WAT, we performed an immunohistochemistry of UCP-1 in WAT and BAT. Consistent with the previous study (17) MCH did not affect UCP1 levels (Supplementary Figure 4). Since MCH also impairs glucose tolerance (4; 14), we next sought to investigate if ARC SIRT1 is involved in the effects of central MCH on glucose metabolism. Indeed, we found that the chronic central infusion of MCH caused glucose intolerance, but this action was blunted in rats that have SIRT1 genetically inhibited in the ARC (Figures 5D-5E). In order to assess if hypothalamic SIRT1 was also an essential mediator of the hepatic actions of MCH, we measured the hepatic TG content. In agreement with previous reports (13; 17) the central treatment with MCH augmented the amount of TG in the liver, and this effect was still persistent when ARC SIRT1 was down-regulated (Figure 5F), indicating that SIRT1 does not mediate the central actions of MCH on hepatic lipid metabolism.

Next, we evaluated the role of the transcription factor FoxO1 as the downstream mediator of SIRT1-dependent MCH action on adipocyte metabolism and glucose intolerance, following a similar setting than the aforementioned for SIRT1. As expected, chronic central infusion of MCH induced significant weight gain (Figure 6A), hyperphagia (Figure 6B), decreased WAT pHSL and pJNK levels and increased WAT CIDEA (Figure 6C) and caused glucose intolerance (Figures 6D and 6E). Notably, all these MCH-induced effects were blunted in rats where FoxO1 was down-regulated in the ARC (Figures 6A-6E) independently of BAT thermogenesis or browning of WAT (Supplementary Figure 4).

Inhibition of SIRT1 in POMC neurons compromises the MCH-induced feeding, body weight gain and adiposity

Since inhibition of SIRT1 in the ARC impairs the anabolic actions of MCH and MCH inhibits POMC neuronal activity, we hypothesized that specific inhibition of SIRT1 in POMC neurons could impair MCH function. To test this, we silenced SIRT1 specifically in POMC neurons by injecting AAV8-hSyn-shSIRT1-DIO-GFP into the MBH of POMC-IRES-Cre mice. Our results showed the specificity of the infection because GFP staining was restricted to POMC neurons (Figure 7A). Three weeks after transfection, mini osmotic pumps were implanted in mice to deliver icv MCH or vehicle (saline) for one week. Chronic central infusion of MCH induced significant reduction of MBH acetyl-p53 levels (Figure 7B), weight gain (Figure 7C), hyperphagia (Figure 7D) and adiposity (Figure 7E). Notably, all these MCH-induced effects were blunted after inhibition of SIRT1 in POMC neurons (Figures 7B-7E). Therefore, these data suggest that SIRT1 specifically in POMC neurons mediates the anabolic actions of MCH. In addition, as we pointed in previous experiments, the anabolic role of MCH was independent of the browning of WAT since UCP1 immunostaining was unchanged in all the studied groups (Figures 7F-7H).

SIRT1 mediates MCH-induced weight gain through the SNS

We previously demonstrated a key role of the SNS inhibition in central MCH-induced weight gain and adiposity (17). Therefore, we hypothesized that down-regulation of SIRT1 in the ARC modulate the efferent SNS subserving WAT. For this, we tested the effect of icv MCH on WAT SNA in absence or presence of EX-527, a SIRT1 antagonist, administered icv. We found that: a) icv Ex527 (10ug/rat) stimulated WAT

SNA, b) icv MCH decreased WAT SNA, and c) a dose of icv EX527 that does not change WAT SNA *per se* was able to suppress the MCH-induced effect on WAT SNA (Figure 7).

Genetic inhibition of central MCH decreases feeding and body weight in wild type but not in SIRT1 transgenic mice

Central injection of MCH-ASO at different doses (1, 2 and 4 nmol/mouse) decreased food intake and body weight in mice fed a chow diet (Figures 8A-8B). Next, we challenged WT mice and mice over-expressing SIRT1 with 60% high fat diet (HFD) for 12 weeks. In WT mice fed a HFD, central administration of MCH-ASO caused a significant decrease in food intake and body weight (Figures 8C-8D), associated with a decrease in hypothalamic mediobasal FoxO1 levels (Figure 8E). However, central MCH-ASO injection to obese SIRT1 transgenic (Tg) mice failed to alter feeding behavior, body weight or hypothalamic FoxO1 levels [after 24 hours](#) (Figures 8F-8H). The injection of MCH-ASO decreased MCH protein levels in both WT and SIRT1 Tg mice [after 24 hours](#) ([Supplementary Figures 5A-5B](#)).

Discussion

Here, we describe for the first time that MCH inhibit the electrical activity of POMC neurons and that SIRT1/FoxO1 mediate the MCH control of food intake, adipocyte lipid storage and glucose metabolism. The central melanocortin system interacts with SIRT1 to modulate energy homeostasis and insulin sensitivity. Pharmacological or genetic inhibition of hypothalamic SIRT1 decrease food intake and weight gain and central administration of a specific melanocortin antagonist, SHU9119, reversed the anorectic

effect of hypothalamic SIRT1 inhibition (35). Mice lacking SIRT1 in POMC neurons were more prone to DIO (37) and selective lack of SIRT1 in hypothalamic AgRP neurons decrease food intake, fat mass and body weight (36). We therefore hypothesized that hypothalamic SIRT1 might govern the metabolic actions of MCH. We focused our attention on the ARC based on the evidence identifying this hypothalamic area as the site where MCH acts to increase food intake and adipocyte lipid deposition (17). Mechanistic studies using pharmacological approach and viral vectors show that down-regulation of SIRT1 in the ARC blunts MCH-induced feeding. Accordingly, genetic silencing of SIRT1 in the ARC blunted adipocyte lipid storage and glucose intolerance caused by chronic central infusion of MCH. Although central MCH favors hepatic lipid deposition (13; 17), this action occurs in the LHA (17), but remained unaltered after inhibition of SIRT1 in the ARC, indicating the specificity of the MCH-SIRT1 pathway. [Therefore, this data indicates that SIRT1 is as a mediator of the anabolic effects of MCH.](#) Furthermore, the role of SIRT1 as a mediator of MCH is consistent with other reports suggesting that hypothalamic SIRT1 mediates the orexigenic action of ghrelin (36; 47).

The SNS connects hypothalamic centers with the WAT, and we previously demonstrated that central MCH control adiposity through the SNS (17). Furthermore, hypothalamic SIRT1 modulates WAT SNA (37). Our findings show that whereas icv MCH decreased WAT SNA, central blockade of SIRT1 blunted this effect. In line with this, the actions of ARC SIRT1 as a modulator of MCH-induced adiposity could be controlled by the administration of a β -adrenoreceptor antagonist, indicating that WAT SNA is a downstream effector of SIRT1. Overall, these results indicate that hypothalamic SIRT1 requires the SNS to modulate the actions of MCH on body fat

mass. Thus, the central MCH/SIRT1 pathway represents a new neuronal circuit of the brain-WAT axis. The increased SIRT1 activity following MCH administration may at first seem counterintuitive, but there are several reports that studied the role of SIRT1 in the hypothalamus and the results are somehow controversial. While deletion of SIRT1 in POMC neurons causes a higher sensitivity to develop obesity when mice are fed a high fat diet (Ramadori G et al, *Cell Metabolism* 2010), we and others reported that ghrelin, a metabolic hormone, which similarly to MCH stimulates feeding and adiposity, and also inhibits the SNA in the WAT, requires hypothalamic SIRT1 to exert its effects (36; 47). Similarly, previous experimental evidence has shown that pharmacological inhibition of SIRT1 at the central level inhibits ghrelin-induced food intake and body weight through the regulation of the FOXO1 and the melanocortin system, including increased levels of acetyl-Foxo1 and POMC expression (35; 36; 48). Thus, further studies are necessary to clarify the role of hypothalamic SIRT1.

Importantly, our studies have identified FoxO1 as critical mechanism within the ARC by which the MCH-SIRT1 pathway controls food intake, adipocyte metabolism and glucose intolerance. Among the large list of molecules that are directly regulated by SIRT1, FoxO1 emerged as a potential candidate because of its interaction with the hypothalamic melanocortin system (49) and in mediating the metabolic effects of central SIRT1 (35). MCH administered icv or directly into the ARC upregulated hypothalamic protein levels of FoxO1, whereas genetic inhibition of ARC SIRT1 abolished this effect. Similarly, to the results obtained with SIRT1, down-regulation of FoxO1 in the ARC blunted MCH-induced feeding, adipocyte lipid storage and glucose intolerance.

To gain insights in the pathophysiological relevance of MCH/SIRT1/FoxO1 pathway in obesity, we injected MCH-ASO centrally, which decreased both food intake and weight

gain in wild type mice fed a chow diet or HFD. Icv MCH-ASO decreased hypothalamic levels of FoxO1 in wild type mice fed a HFD. However, central MCH-ASO failed to modify food intake or body weight in mice over-expressing SIRT1. This lack of effect was associated with inability of MCH-ASO to inhibit hypothalamic FoxO1. Finally, the interaction between the MCH system and SIRT1/FoxO1 appears to occur in POMC neurons. This is demonstrated because when we disrupt GABA signaling into the ARC neurons, [which is the neurotransmitter in charge of the neural communication between AgRP and POMC neurons](#), central MCH is still able to stimulate feeding. Indeed, POMC neurons receive also inhibitory inputs from outside the ARC (40), but this results together with the fact that MCH-ASO maintained their hypophagic action after the chemogenetic stimulation of AgRP neurons, suggests that AgRP neurons fail to significantly influence MCH-mediated feeding. [Moreover](#), our functional data showed that MCH dramatically inhibits spontaneous neuronal activity in a significant subset of POMC neurons. Indeed, we obtained certain variability in the response of these neurons, which was expected due to the high heterogeneity of POMC neurons [based on their molecular taxonomy, neurotransmitter and receptor expression](#) (50). [Lastly, our hypothesis was countersigned/confirmed by the fact that the virogenetic deletion of SIRT1 specifically in POMC neurons blunted the actions of MCH. We found that in mice lacking SIRT1 in POMC neurons, MCH is less effective in inducing weight gain, feeding and adiposity compared to mice with intact SIRT1 expression in those neurons. The incomplete blockade of MCH actions in our animal model might be explained by the fact that the adenoviral vector did not infect all MCH-R-expressing POMC neurons, and that some of the infected POMC neurons likely did not express MCH-R. This is in concordance with the aforementioned heterogeneity of POMC neurons.](#) Overall, our

findings conclusively suggest the key involvement of these neurons in MCH-mediated effects in the ARC.

In summary, our data highlight the relevance of the MCH system as a drug target and provide new conceptual framework on the mechanisms by which MCH modulates food intake, adipocyte lipid storage and glucose intolerance via a SIRT1/FoxO1 in the ARC. This mechanism requires POMC but not AgRP neurons and is essential for the activity of MCH inhibitors in obesity.

AUTHORS CONTRIBUTIONS

O.A-M, M.Q., [A.R-P.](#), [C.F.](#), [A.S.](#), R.H.B., S.C.F., M.I., D.B. performed *in vivo* experiments and western blots and collected and analyzed the data. D.A.M and K.R. performed and analyzed the sympathetic nerve activity recording studies. J.C. performed and analyzed electrophysiological recordings from brain slices. B.Y.H.L. and G.Y. performed FACS and RNAseq. R.G., L.G-C., I.K., Z.L [and V. H.](#) performed the I.H.C. images. Y.S., M.F. and M.J.C. contributed to the development of the analytical tools, reagents and discussion. O.A-M, M.Q, M.J.K., S.L., M.L., Z.L., V.P., K.R., C.D. and R.N. designed the experiments and discussed the manuscript. I.K., Z.L., D.A.M., K.R., O.A-M., M.Q. and J.C. made the figures. O.A-M., M.Q. and R.N. wrote the manuscript. C.D. and R.N. coordinated and directed the project and developed the hypothesis.

Acknowledgements

The authors thank Manuel Serrano (CNIO, Spain) for providing SIRT1-tg mice, Jens Bruning (Max Planck Institute for Metabolism Research, Germany) and Eleftheria Maratos-Flier (Beth Israel Deaconess Medical Center, USA) for providing AgRP-Cre and Mchr1-cre/tdTomato transgene mice respectively and critical reading. This work was supported by grants from Ministerio de Economía y Competitividad (ML: SAF2015-71026-R; CD: [BFU2017-87721](#); RN: BFU2015-70664R), [Consellería de Cultura, Educación e Ordenación Universitaria, Xunta de Galicia \(ML: 2015-CP079 and 2016-PG068; R.N.: 2015-CP080, 2016-PG057 and Centro singular de investigación de Galicia accreditation 2016-2019, ED431G/05\) and the European Regional Development Fund \(ERDF\).](#) Fundación Atresmedia (ML and RN), BBVA Foundation

(RN) and the National Science Foundation of Hungary (OTKA K101326, K100722). KR work is supported by US National Institutes of Health (HL084207), American Heart Association (EIA#14EIA18860041), [the Veterans Affairs \(BX004249\)](#) and The University of Iowa Fraternal Order of Eagles Diabetes Research Center. Centro de Investigación Biomédica en Red (CIBER) de Fisiopatología de la Obesidad y Nutrición (CIBERobn). CIBERobn is an initiative of the Instituto de Salud Carlos III (ISCIII) of Spain which is supported by FEDER funds. M.Q. is a recipient of a Postdoctoral contract from Galician Government (Xunta de Galicia ED481B2018/004). J.C. was supported by Marie Skłodowska-Curie Actions– European Research Fellowship (H2020-MSCA-IF-2014, ID656657) and Région Hauts-de-France (program VisionAIRR). O.AM is funded by the ISCIII/SERGAS through a research contract “Sara Borrell” (CD14/00091). R.N. is the guarantor of this work and, as such, had full access to all the data in the study and take responsibility for the integrity of the data and the accuracy of the data analysis.

Conflict of interest

The authors declare that they have no conflicts of interest

References

1. Pissios P, Bradley RL, Maratos-Flier E: Expanding the scales: The multiple roles of MCH in regulating energy balance and other biological functions. *Endocrine reviews* 2006;27:606-620
2. Kawauchi H, Abe K, Takahashi A, Hirano T, Hasegawa S, Naito N, Nakai Y: Isolation and properties of chum salmon prolactin. *General and comparative endocrinology* 1983;49:446-458
3. Qu D, Ludwig DS, Gammeltoft S, Piper M, Pelleymounter MA, Cullen MJ, Mathes WF, Przypek R, Kanarek R, Maratos-Flier E: A role for melanin-concentrating hormone in the central regulation of feeding behaviour. *Nature* 1996;380:243-247
4. Ludwig DS, Tritos NA, Mastaitis JW, Kulkarni R, Kokkotou E, Elmquist J, Lowell B, Flier JS, Maratos-Flier E: Melanin-concentrating hormone overexpression in transgenic mice leads to obesity and insulin resistance. *The Journal of clinical investigation* 2001;107:379-386
5. Ito M, Ishihara A, Gomori A, Egashira S, Matsushita H, Mashiko S, Ito J, Ito M, Nakase K, Haga Y, Iwaasa H, Suzuki T, Ohtake N, Moriya M, Sato N, MacNeil DJ, Takenaga N, Tokita S, Kanatani A: Melanin-concentrating hormone 1-receptor antagonist suppresses body weight gain correlated with high receptor occupancy levels in diet-induced obesity mice. *European journal of pharmacology* 2009;624:77-83
6. Shearman LP, Camacho RE, Sloan Stribling D, Zhou D, Bednarek MA, Hreniuk DL, Feighner SD, Tan CP, Howard AD, Van der Ploeg LH, MacIntyre DE, Hickey GJ, Strack AM: Chronic MCH-1 receptor modulation alters appetite, body weight and adiposity in rats. *European journal of pharmacology* 2003;475:37-47
7. Mashiko S, Ishihara A, Gomori A, Moriya R, Ito M, Iwaasa H, Matsuda M, Feng Y, Shen Z, Marsh DJ, Bednarek MA, MacNeil DJ, Kanatani A: Antiobesity effect of a melanin-concentrating hormone 1 receptor antagonist in diet-induced obese mice. *Endocrinology* 2005;146:3080-3086
8. Shimada M, Tritos NA, Lowell BB, Flier JS, Maratos-Flier E: Mice lacking melanin-concentrating hormone are hypophagic and lean. *Nature* 1998;396:670-674
9. Segal-Lieberman G, Bradley RL, Kokkotou E, Carlson M, Trombly DJ, Wang X, Bates S, Myers MG, Jr., Flier JS, Maratos-Flier E: Melanin-concentrating hormone is a critical mediator of the leptin-deficient phenotype. *Proceedings of the National Academy of Sciences of the United States of America* 2003;100:10085-10090
10. Alon T, Friedman JM: Late-onset leanness in mice with targeted ablation of melanin concentrating hormone neurons. *The Journal of neuroscience : the official journal of the Society for Neuroscience* 2006;26:389-397
11. Kokkotou E, Jeon JY, Wang X, Marino FE, Carlson M, Trombly DJ, Maratos-Flier E: Mice with MCH ablation resist diet-induced obesity through strain-specific mechanisms. *American journal of physiology Regulatory, integrative and comparative physiology* 2005;289:R117-124
12. Jeon JY, Bradley RL, Kokkotou EG, Marino FE, Wang X, Pissios P, Maratos-Flier E: MCH^{-/-} mice are resistant to aging-associated increases in body weight and insulin resistance. *Diabetes* 2006;55:428-434
13. Wang Y, Ziogas DC, Biddinger S, Kokkotou E: You deserve what you eat: lessons learned from the study of the melanin-concentrating hormone (MCH)-deficient mice. *Gut* 2010;59:1625-1634
14. Pereira-da-Silva M, De Souza CT, Gasparetti AL, Saad MJ, Velloso LA: Melanin-concentrating hormone induces insulin resistance through a mechanism independent of body weight gain. *The Journal of endocrinology* 2005;186:193-201
15. Kong D, Vong L, Parton LE, Ye C, Tong Q, Hu X, Choi B, Bruning JC, Lowell BB: Glucose stimulation of hypothalamic MCH neurons involves K(ATP) channels, is modulated by UCP2, and regulates peripheral glucose homeostasis. *Cell metabolism* 2010;12:545-552
16. Domingos AI, Sordillo A, Dietrich MO, Liu ZW, Tellez LA, Vaynshteyn J, Ferreira JG, Ekstrand MI, Horvath TL, de Araujo IE, Friedman JM: Hypothalamic melanin concentrating hormone neurons communicate the nutrient value of sugar. *eLife* 2013;2:e01462
17. Imbernon M, Beiroa D, Vazquez MJ, Morgan DA, Veyrat-Durebex C, Porteiro B, Diaz-Arteaga A, Senra A, Busquets S, Velasquez DA, Al-Massadi O, Varela L, Gandara M, Lopez-Soriano FJ, Gallego R, Seoane LM, Argiles JM, Lopez M, Davis RJ, Sabio G, Rohner-

- Jeanrenaud F, Rahmouni K, Dieguez C, Nogueiras R: Central melanin-concentrating hormone influences liver and adipose metabolism via specific hypothalamic nuclei and efferent autonomic/JNK1 pathways. *Gastroenterology* 2013;144:636-649 e636
18. Saito Y, Nothacker HP, Wang Z, Lin SH, Leslie F, Civelli O: Molecular characterization of the melanin-concentrating-hormone receptor. *Nature* 1999;400:265-269
19. Marsh DJ, Weingarth DT, Novi DE, Chen HY, Trumbauer ME, Chen AS, Guan XM, Jiang MM, Feng Y, Camacho RE, Shen Z, Frazier EG, Yu H, Metzger JM, Kuca SJ, Shearman LP, Gopal-Truter S, MacNeil DJ, Strack AM, MacIntyre DE, Van der Ploeg LH, Qian S: Melanin-concentrating hormone 1 receptor-deficient mice are lean, hyperactive, and hyperphagic and have altered metabolism. *Proceedings of the National Academy of Sciences of the United States of America* 2002;99:3240-3245
20. Chen Y, Hu C, Hsu CK, Zhang Q, Bi C, Asnicar M, Hsiung HM, Fox N, Sliker LJ, Yang DD, Heiman ML, Shi Y: Targeted disruption of the melanin-concentrating hormone receptor-1 results in hyperphagia and resistance to diet-induced obesity. *Endocrinology* 2002;143:2469-2477
21. Chee MJ, Pissios P, Maratos-Flier E: Neurochemical characterization of neurons expressing melanin-concentrating hormone receptor 1 in the mouse hypothalamus. *The Journal of comparative neurology* 2013;521:2208-2234
22. Saito Y, Cheng M, Leslie FM, Civelli O: Expression of the melanin-concentrating hormone (MCH) receptor mRNA in the rat brain. *The Journal of comparative neurology* 2001;435:26-40
23. Bittencourt AL, Barral A, Costa JM, Saldanha AC, Badaro F, Barral-Netto M, Freitas LA: Diffuse cutaneous leishmaniasis with atypical aspects. *International journal of dermatology* 1992;31:568-570
24. Nahon JL, Presse F, Bittencourt JC, Sawchenko PE, Vale W: The rat melanin-concentrating hormone messenger ribonucleic acid encodes multiple putative neuropeptides coexpressed in the dorsolateral hypothalamus. *Endocrinology* 1989;125:2056-2065
25. Skofitsch G, Jacobowitz DM, Zamir N: Immunohistochemical localization of a melanin concentrating hormone-like peptide in the rat brain. *Brain research bulletin* 1985;15:635-649
26. Guyon A, Conductier G, Rovere C, Enfissi A, Nahon JL: Melanin-concentrating hormone producing neurons: Activities and modulations. *Peptides* 2009;30:2031-2039
27. Ludwig DS, Mountjoy KG, Tatro JB, Gillette JA, Frederich RC, Flier JS, Maratos-Flier E: Melanin-concentrating hormone: a functional melanocortin antagonist in the hypothalamus. *The American journal of physiology* 1998;274:E627-633
28. Tritos NA, Vicent D, Gillette J, Ludwig DS, Flier ES, Maratos-Flier E: Functional interactions between melanin-concentrating hormone, neuropeptide Y, and anorectic neuropeptides in the rat hypothalamus. *Diabetes* 1998;47:1687-1692
29. Chaffer CL, Morris MJ: The feeding response to melanin-concentrating hormone is attenuated by antagonism of the NPY Y(1)-receptor in the rat. *Endocrinology* 2002;143:191-197
30. Nogueiras R, Habegger KM, Chaudhary N, Finan B, Banks AS, Dietrich MO, Horvath TL, Sinclair DA, Pfluger PT, Tschop MH: Sirtuin 1 and sirtuin 3: physiological modulators of metabolism. *Physiological reviews* 2012;92:1479-1514
31. Chalkiadaki A, Guarente L: Sirtuins mediate mammalian metabolic responses to nutrient availability. *Nature reviews Endocrinology* 2012;8:287-296
32. Haigis MC, Sinclair DA: Mammalian sirtuins: biological insights and disease relevance. *Annual review of pathology* 2010;5:253-295
33. Coppari R: Metabolic actions of hypothalamic SIRT1. *Trends in endocrinology and metabolism: TEM* 2012;23:179-185
34. Toorie AM, Nillni EA: Minireview: Central Sirt1 regulates energy balance via the melanocortin system and alternate pathways. *Molecular endocrinology* 2014;28:1423-1434
35. Cakir I, Perello M, Lansari O, Messier NJ, Vaslet CA, Nillni EA: Hypothalamic Sirt1 regulates food intake in a rodent model system. *PloS one* 2009;4:e8322
36. Dietrich MO, Antunes C, Geliang G, Liu ZW, Borok E, Nie Y, Xu AW, Souza DO, Gao Q, Diano S, Gao XB, Horvath TL: Agrp neurons mediate Sirt1's action on the melanocortin system

- and energy balance: roles for Sirt1 in neuronal firing and synaptic plasticity. *J Neurosci* 2010;30:11815-11825
37. Ramadori G, Fujikawa T, Fukuda M, Anderson J, Morgan DA, Mostoslavsky R, Stuart RC, Perello M, Vianna CR, Nillni EA, Rahmouni K, Coppari R: SIRT1 deacetylase in POMC neurons is required for homeostatic defenses against diet-induced obesity. *Cell metabolism* 2010;12:78-87
38. Clasadonte J, Scemes E, Wang Z, Boison D, Haydon PG: Connexin 43-Mediated Astroglial Metabolic Networks Contribute to the Regulation of the Sleep-Wake Cycle. *Neuron* 2017;95:1365-1380 e1365
39. Imbernon M, Sanchez-Rebordelo E, Romero-Pico A, Kallo I, Chee MJ, Porteiro B, Al-Massadi O, Contreras C, Ferno J, Senra A, Gallego R, Folgueira C, Seoane LM, van Gestel M, Adan RA, Liposits Z, Dieguez C, Lopez M, Nogueiras R: Hypothalamic kappa opioid receptor mediates both diet-induced and melanin concentrating hormone-induced liver damage through inflammation and endoplasmic reticulum stress. *Hepatology* 2016;64:1086-1104
40. Atasoy D, Betley JN, Su HH, Sternson SM: Deconstruction of a neural circuit for hunger. *Nature* 2012;488:172-177
41. Quinones M, Al-Massadi O, Gallego R, Ferno J, Dieguez C, Lopez M, Nogueiras R: Hypothalamic CaMKKbeta mediates glucagon anorectic effect and its diet-induced resistance. *Molecular metabolism* 2015;4:961-970
42. Quinones M, Al-Massadi O, Folgueira C, Bremser S, Gallego R, Torres-Leal L, Haddad-Tovoli R, Garcia-Caceres C, Hernandez-Bautista R, Lam BYH, Beiroa D, Sanchez-Rebordelo E, Senra A, Malagon JA, Valerio P, Fondevila MF, Ferno J, Malagon MM, Contreras R, Pfluger P, Bruning JC, Yeo G, Tschop M, Dieguez C, Lopez M, Claret M, Kloppenburg P, Sabio G, Nogueiras R: p53 in AgRP neurons is required for protection against diet-induced obesity via JNK1. *Nature communications* 2018;9:3432
43. Martinez de Morentin PB, Gonzalez-Garcia I, Martins L, Lage R, Fernandez-Mallo D, Martinez-Sanchez N, Ruiz-Pino F, Liu J, Morgan DA, Pinilla L, Gallego R, Saha AK, Kalsbeek A, Fliers E, Bisschop PH, Dieguez C, Nogueiras R, Rahmouni K, Tena-Sempere M, Lopez M: Estradiol regulates brown adipose tissue thermogenesis via hypothalamic AMPK. *Cell metabolism* 2014;20:41-53
44. Imbernon M, Sanchez-Rebordelo E, Gallego R, Gandara M, Lear P, Lopez M, Dieguez C, Nogueiras R: Hypothalamic KLF4 mediates leptin's effects on food intake via AgRP. *Molecular metabolism* 2014;3:441-451
45. Mandelblat-Cerf Y, Ramesh RN, Burgess CR, Patella P, Yang Z, Lowell BB, Andermann ML: Arcuate hypothalamic AgRP and putative POMC neurons show opposite changes in spiking across multiple timescales. *eLife* 2015;4
46. Zhan C, Zhou J, Feng Q, Zhang JE, Lin S, Bao J, Wu P, Luo M: Acute and long-term suppression of feeding behavior by POMC neurons in the brainstem and hypothalamus, respectively. *The Journal of neuroscience : the official journal of the Society for Neuroscience* 2013;33:3624-3632
47. Velasquez DA, Martinez G, Romero A, Vazquez MJ, Boit KD, Dopeso-Reyes IG, Lopez M, Vidal A, Nogueiras R, Dieguez C: The central Sirtuin 1/p53 pathway is essential for the orexigenic action of ghrelin. *Diabetes* 2011;60:1177-1185
48. Cyr NE, Steger JS, Toorie AM, Yang JZ, Stuart R, Nillni EA: Central Sirt1 regulates body weight and energy expenditure along with the POMC-derived peptide alpha-MSH and the processing enzyme CPE production in diet-induced obese male rats. *Endocrinology* 2015;156:961-974
49. Kitamura T, Feng Y, Kitamura YI, Chua SC, Jr., Xu AW, Barsh GS, Rossetti L, Accili D: Forkhead protein FoxO1 mediates Agrp-dependent effects of leptin on food intake. *Nature medicine* 2006;12:534-540
50. Kim JG, Sun BH, Dietrich MO, Koch M, Yao GQ, Diano S, Insogna K, Horvath TL: AgRP Neurons Regulate Bone Mass. *Cell reports* 2015;13:8-14

Figure legends

Figure 1. Central MCH stimulates hypothalamic FoxO1 levels and down-regulates POMC protein levels through MCH-R in the ARC. Central effects of icv MCH administration (20 μ g/rat) on **(A)** food intake, **(B)** hypothalamic protein levels of acetyl-p53, FoxO1, acetyl-FoxO1 and **(C)** hypothalamic protein levels of AgRP and POMC in rats after 2 hours. **(D)** Fluorescein-isothiocyanate (FITC) staining in the hypothalamic ARC. **(E)** Food intake and **(F)** ARC protein levels of acetyl-p53, FoxO1, acetyl-FoxO1 and POMC in rats 2 hours after injection of MCH directly in the ARC. **(G)** GFP expression in the hypothalamic ARC after stereotaxic injection of shMCHR1 lentivirus. **(H)** Protein levels of MCH-R in the ARC of rats stereotaxically injected with scrambled or shMCHR1 lentiviruses. **(I)** Effect of icv MCH on food intake in rats stereotaxically injected with scrambled or shMCHR1 lentiviruses into the ARC. **(J)** Protein levels of FoxO1 and POMC in the hypothalamic ARC of rats stereotaxically injected with scrambled or shMCHR1 lentiviruses in the ARC and icv MCH. β -actin was used to normalize protein levels. Dividing lines indicate spliced bands from the same gel. Values are mean \pm SEM of 7–10 animals per group.

Figure 2. MCH inhibits the activity of POMC neurons in the ARC. **(A)** FACS sorting and single-cell RNA sequencing of POMC-eGFP neurons showing MCH-R, SIRT1 and FoxO1 expression (GEO Database repository: GEO Accession: GSE92707) **(B)** Left: A spontaneously fluorescent ARC POMC neuron (arrow) from a Pomc-Cre:ROSA-tdTomato mouse was identified for patch-clamp recording. Right: Infrared differential interference contrast (IR-DIC) of the same image showing a patched pipette (dotted lines) placed on the cell membrane of the identified POMC neuron (arrow). Scale bars: 50 μ m. **(C)** Whole-cell current-clamp recording showing that MCH

reversibly decreased the spontaneous firing activity of the POMC neuron patched in (B). Note that the inhibitory effect was accompanied by a membrane hyperpolarization. Denoted regions of the recording are shown underneath with an expanded time scale. (D) Average membrane potential of ARC POMC neurons in control conditions and in the presence of MCH ($***p < 0.001$, paired t test, $n = 6$ cells from 4 mice). (E) Average firing rate of ARC POMC neurons in control conditions and in the presence of MCH ($*p < 0.05$, paired t test, $n = 6$ cells from 4 mice). (F) Trace showing that MCH reduced the spontaneous firing activity of another ARC POMC neuron recorded in loose patch configuration. Pooled data are shown as mean \pm SEM. $*P \leq 0.05$, $**P \leq 0.01$; and $***P \leq 0.001$ vs controls.

Figure 3. Central MCH requires POMC but not AgRP to stimulate feeding. (A) POMC protein levels in the ARC and (B) effect of icv MCH-ASO on food intake in rats stereotaxically injected with scrambled or shPOMC lentiviruses in the ARC. (C) GABA-R protein levels in the ARC and (D) effect of icv MCH on food intake in rats stereotaxically injected with scrambled or shGABA-R lentiviruses in the ARC. (E) mCherry expression in the hypothalamic ARC after stereotaxic injection of hSYN-DIO-Hm3D(Gq)-mCherry AVV. (F) Effect of icv MCH-ASO on food intake in AgRP-CRE mice stereotaxically injected with hSYN-DIO-Hm3D(Gq)-mCherry AVV in the ARC. β -actin was used to normalize protein levels. Dividing lines indicate spliced bands from the same gel. Values are mean \pm SEM of 8–10 animals per group. $*P \leq 0.05$, $**P \leq 0.01$; and $***P \leq 0.001$ vs controls.

Figure 4. Central MCH requires SIRT1 and FoxO1 in the hypothalamic ARC to stimulate feeding. (A) SIRT1 protein levels in the ARC, (B) effect of icv MCH on food intake, and (C) protein levels of FoxO1 and POMC in the hypothalamic ARC of rats stereotaxically injected with scrambled or shSIRT1 lentiviruses in the ARC and icv MCH. (D) FoxO1 protein levels in the ARC, (E) effect of icv MCH on food intake in rats, and (F) protein levels of POMC in the hypothalamic ARC of rats stereotaxically injected with scrambled or shFoxO1 lentiviruses in the ARC and icv MCH. β -actin was used to normalize protein levels. Dividing lines indicate spliced bands from the same gel. Values are mean \pm SEM of 8–10 animals per group. * $P \leq 0.05$, ** $P \leq 0.01$; and *** $P \leq 0.001$ vs controls.

Figure 5. SIRT1 in the ARC is essential for MCH-induced food intake, WAT lipid storage and glucose intolerance. (A) Body weight change, (B) cumulative food intake, (C) WAT protein levels of pHSL, pJNK and CIDEA, (D) glucose tolerance test, (E) area under the curve, and (F) hepatic triglyceride content in rats that received shSIRT1 or GFP scrambled lentiviruses in the ARC followed by chronic icv MCH (10 μ g/day/rat) for 1 week. β -actin was used as loading control. Dividing lines indicate spliced bands from the same gel. Values are mean \pm SEM of 7–10 animals per group. * $P \leq 0.05$, ** $P \leq 0.01$; and *** $P \leq 0.001$ vs controls.

Figure 6. FoxO1 in the ARC is essential for MCH-induced food intake, WAT lipid storage and glucose intolerance. (A) Body weight change, (B) cumulative food intake, (C) WAT protein levels of pHSL, pJNK and CIDEA, (D) glucose tolerance test, and (E) area under the curve in rats that microinjected with shFoxO1 or GFP scrambled lentiviruses into the ARC before icv MCH (10 μ g/day/rat) for 1 week. β -actin was used

as loading control. Dividing lines indicate spliced bands from the same gel. Values are mean \pm SEM of 7–10 animals per group. * $P \leq 0.05$, ** $P \leq 0.01$; and *** $P \leq 0.001$ vs controls.

Figure 7. SIRT1 in the POMC neurons regulates MCH-induced food intake, body weight and WAT lipid storage. Representative immunofluorescence showing GFP and POMC colocalization (A). MBH protein levels of acetyl-p53 and p53 (B). Body weight change (C); cumulative food intake (D); fat mass (E); representative pictures of WAT histology (hematoxylin-eosin) (F), WAT protein levels of UCP1 (G); BAT mass (H). Effect of pre-treatment with vehicle versus SIRT1 antagonist Ex-527 (5 $\mu\text{g}/\text{rat}$ and 10 $\mu\text{g}/\text{rat}$) on WAT SNA response evoked by icv MCH (10 $\mu\text{g}/\text{rat}$) in rats (I); β -actin was used to normalize protein levels. Dividing lines indicate spliced bands from the same gel. Values are mean \pm SEM of 6–10 animals per group. * $P < 0.05$; ** $P < 0.01$ and *** $P < 0.001$ vs controls.

Figure 8. Over-expression of SIRT1 blunts MCH-ASO-induced hypophagia. Effect of icv MCH-ASO (1, 2 and 4 nmol/mouse) on (A) food intake and (B) body weight change in wild type mice fed a chow diet. Effect of icv MCH-ASO (1, 2 and 4 nmol/mouse) on (C) food intake, (D) body weight change, and (E) protein levels of FoxO1 in the MBH of wild type mice fed a high fat diet (HFD). Effect of icv ASO-MCH (2 nmol/mouse) on (F) food intake, (G) body weight change, and (H) protein levels of FoxO1 in the MBH of SIRT1 transgenic (Tg) mice fed a HFD. β -actin was used to normalize protein levels. Dividing lines indicate spliced bands from the same gel. Values are mean \pm SEM of 6–10 animals per group. * $P \leq 0.05$ vs controls. Values

are mean \pm SEM of 6–10 animals per group. $*P \leq 0.05$; **P < 0.01 and ***P < 0.001 vs controls.

Figure 1

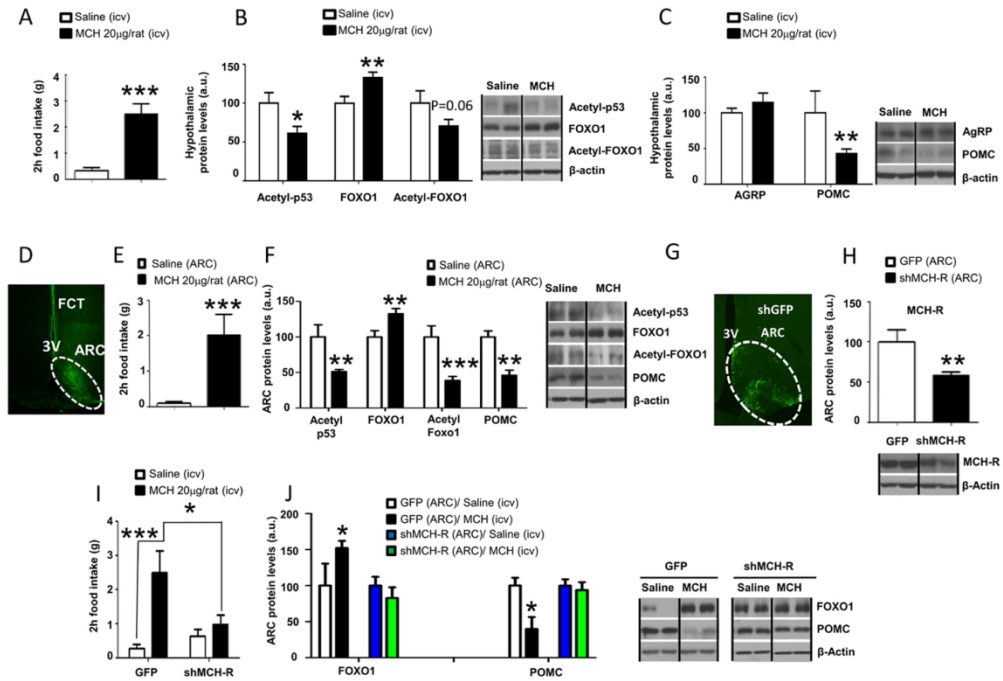
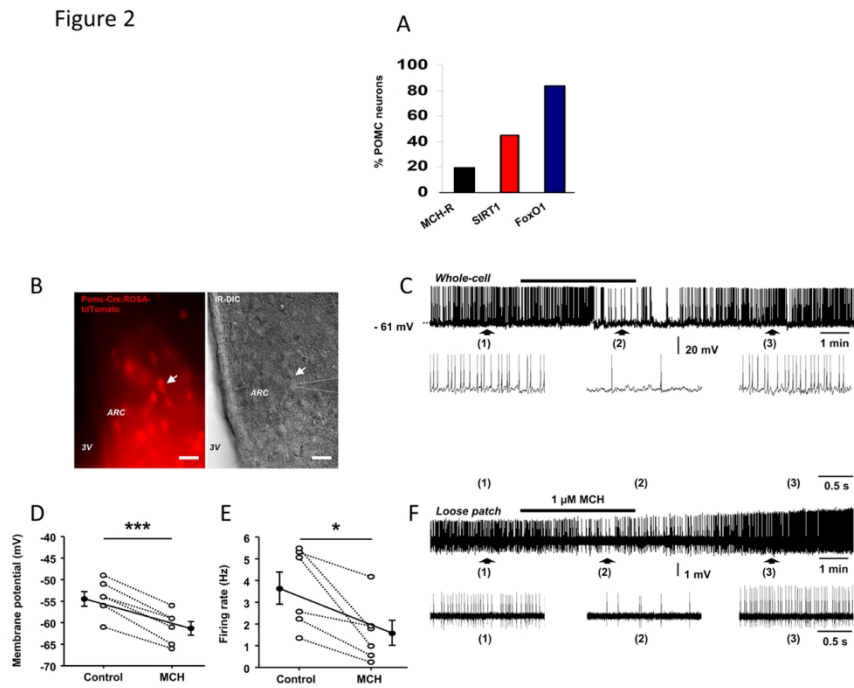


Figure 1

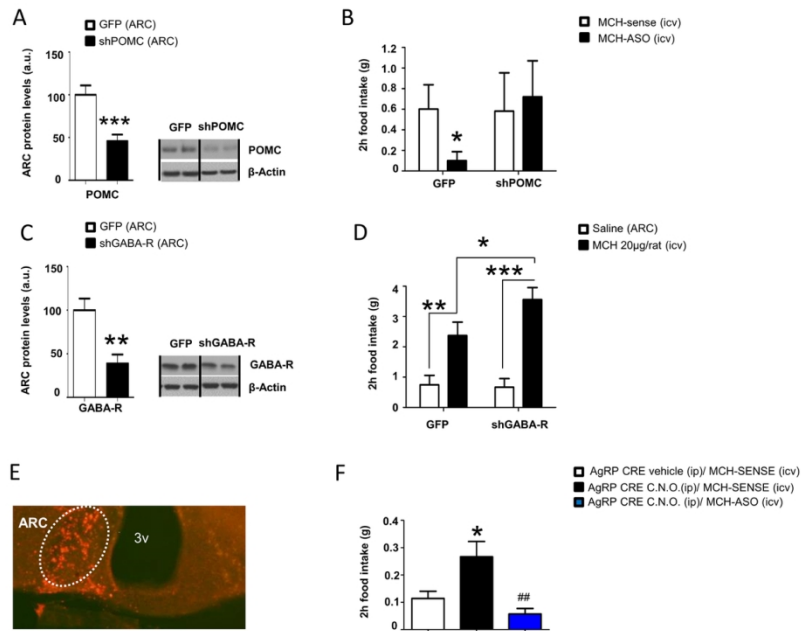
66x49mm (600 x 600 DPI)

Figure 2



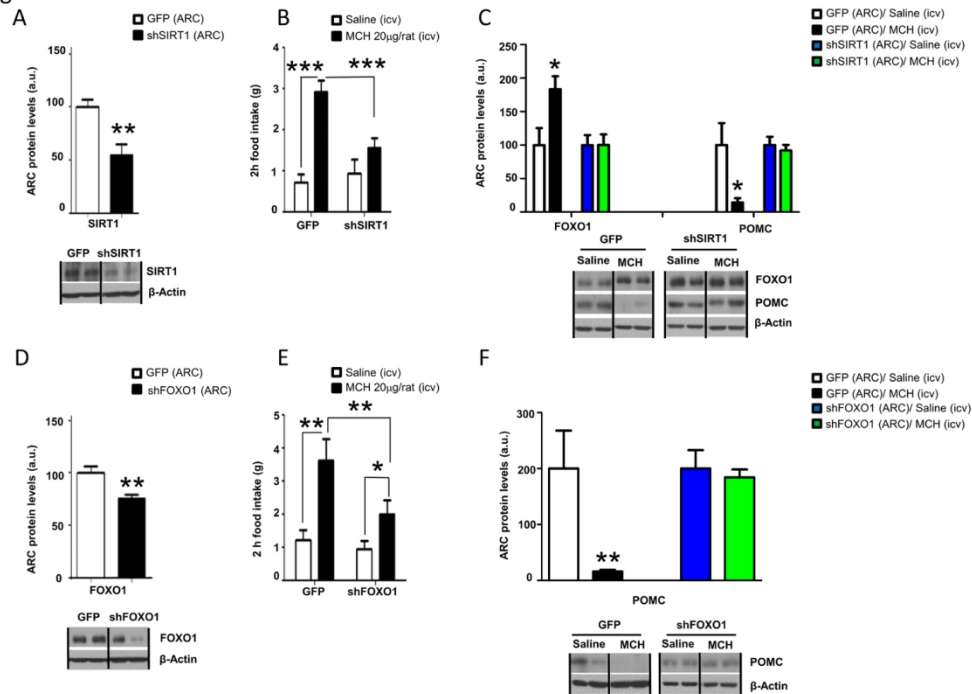
66x49mm (600 x 600 DPI)

Figure 3

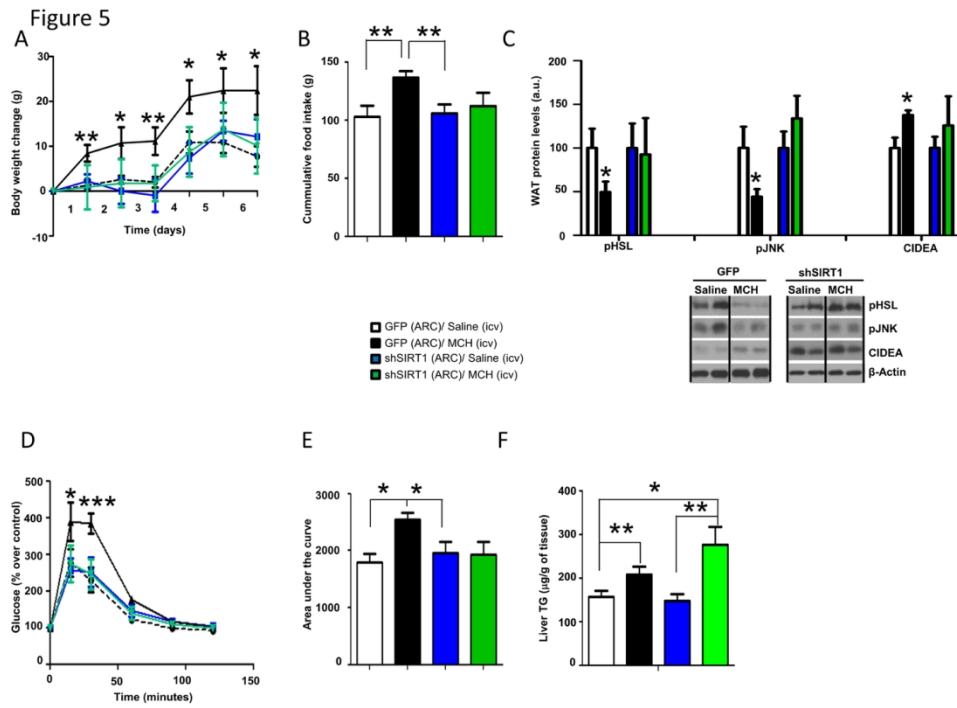


66x49mm (600 x 600 DPI)

Figure 4



66x49mm (600 x 600 DPI)



66x49mm (600 x 600 DPI)

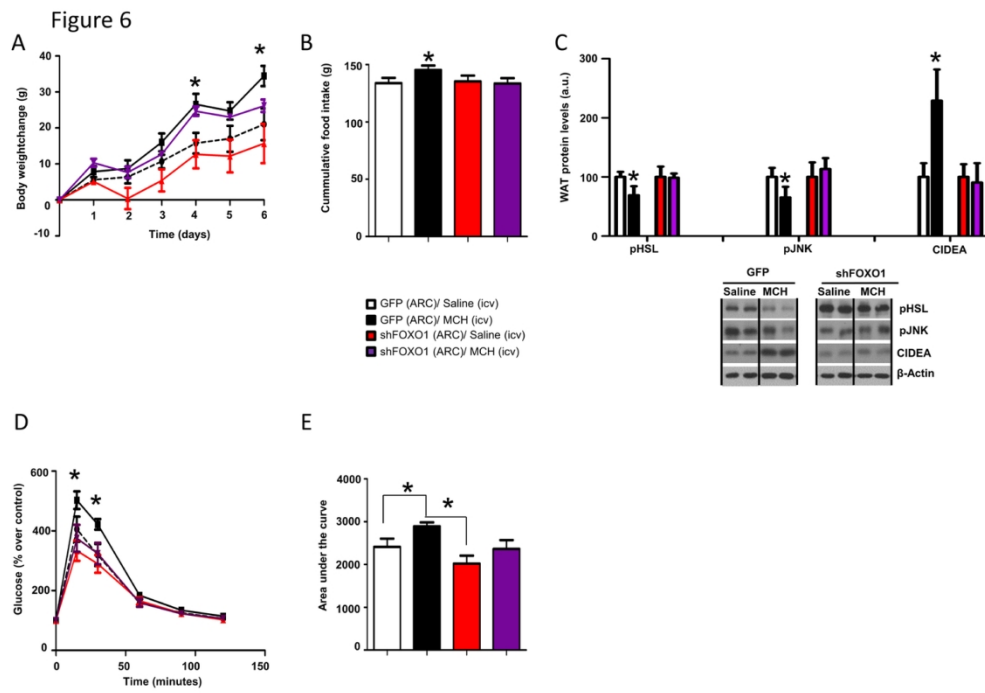


Figure 6

66x49mm (600 x 600 DPI)

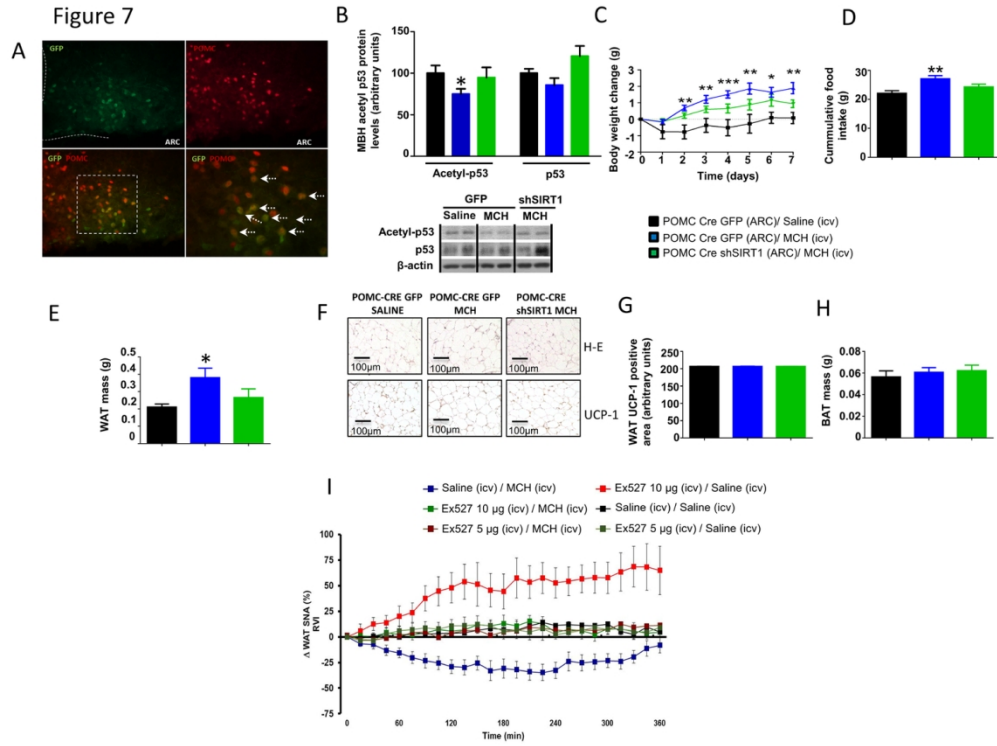


Figure 7

66x49mm (600 x 600 DPI)

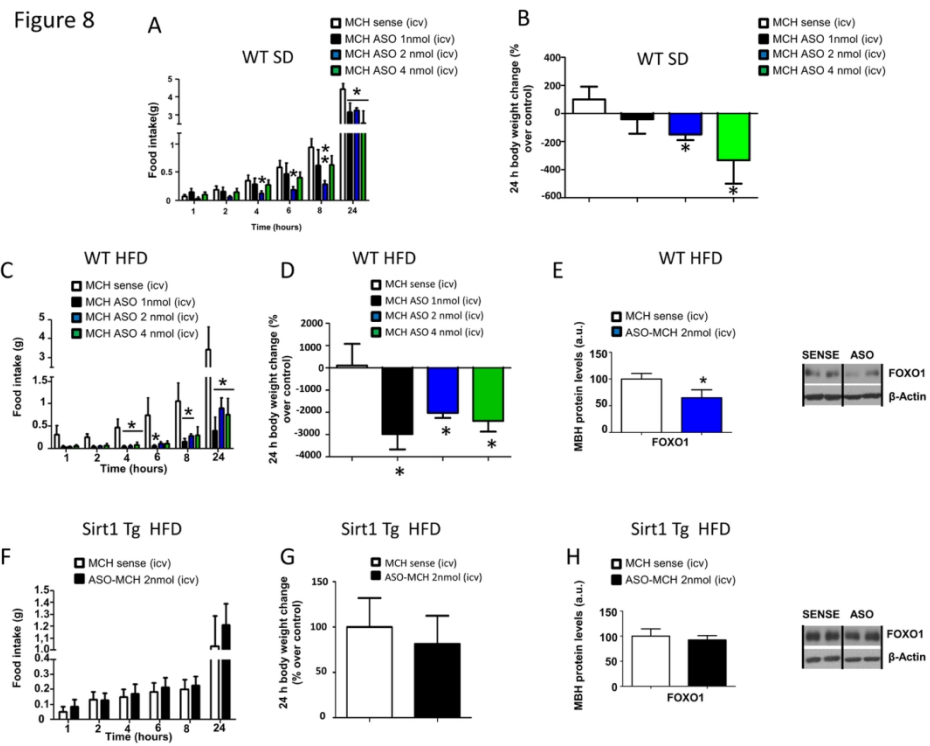
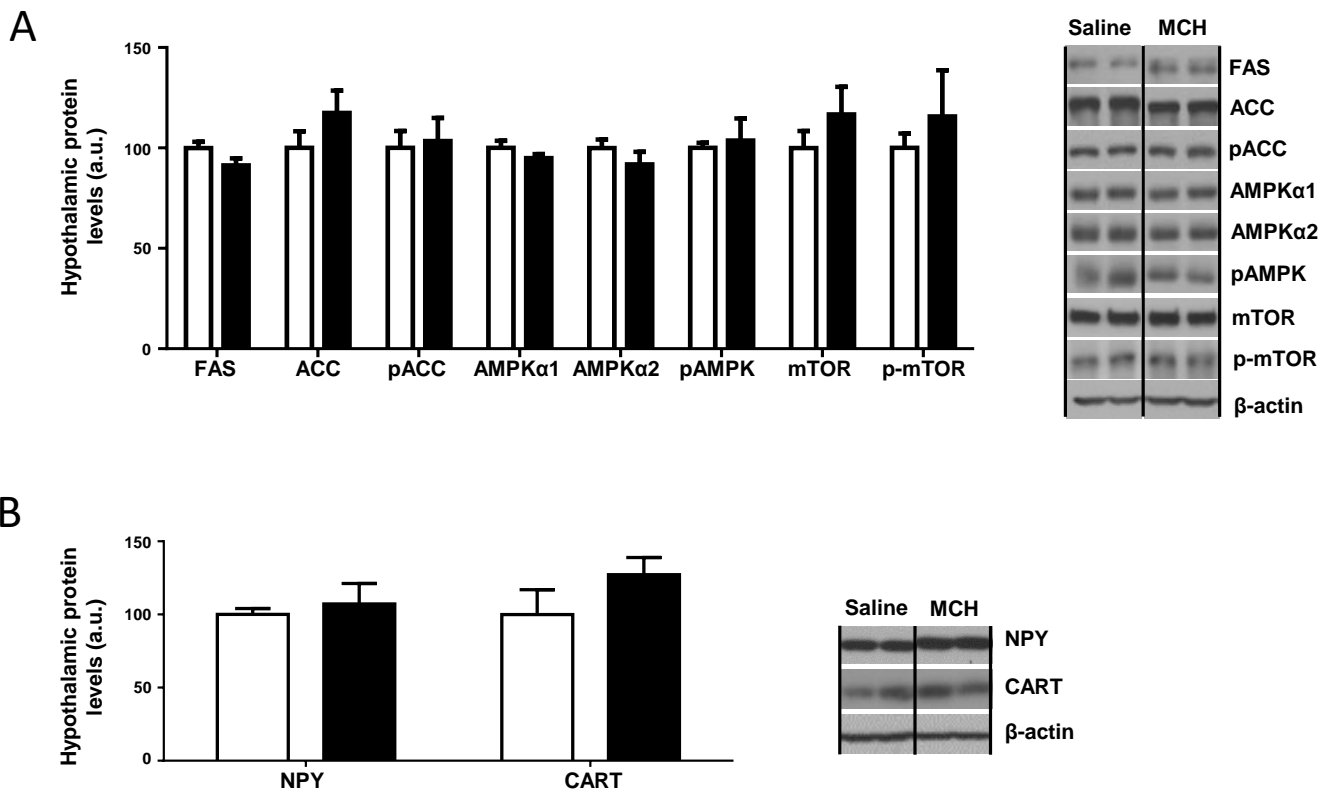


Figure 8

66x49mm (600 x 600 DPI)

Figure S1



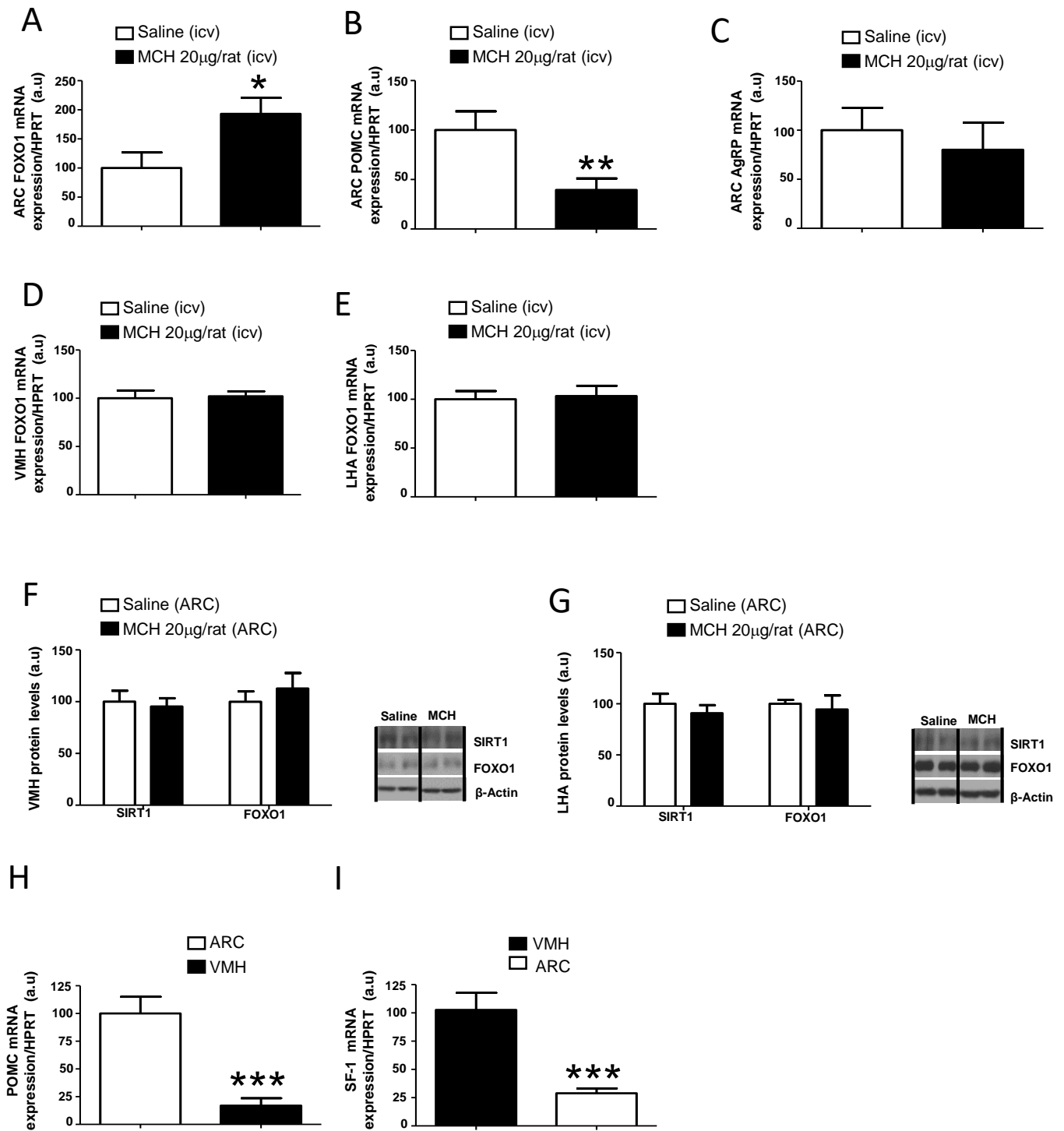
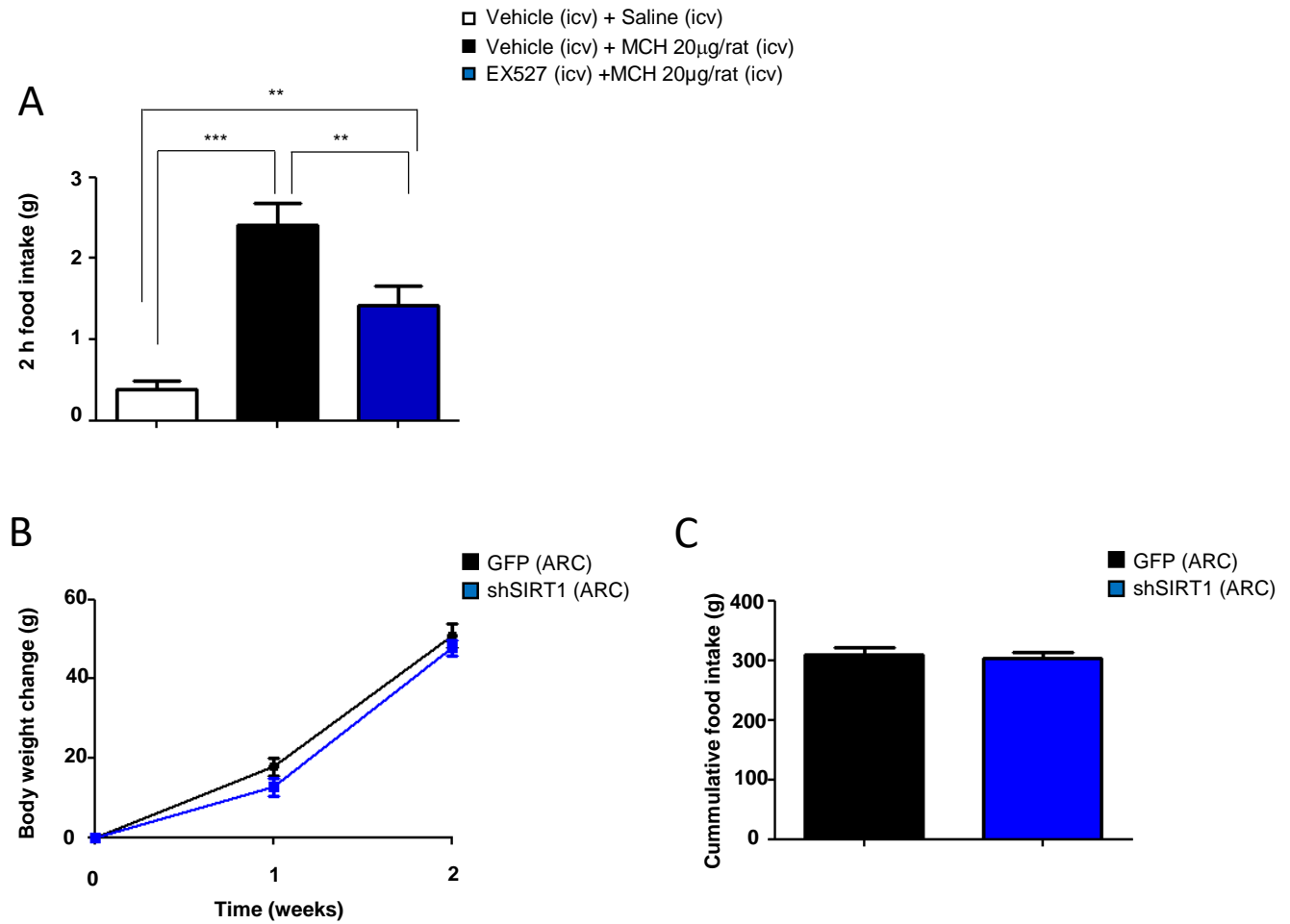
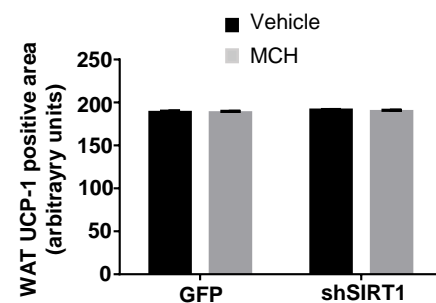
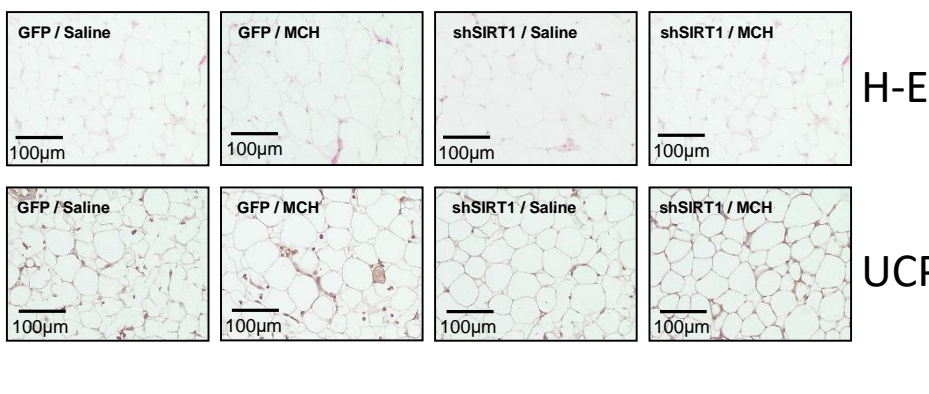


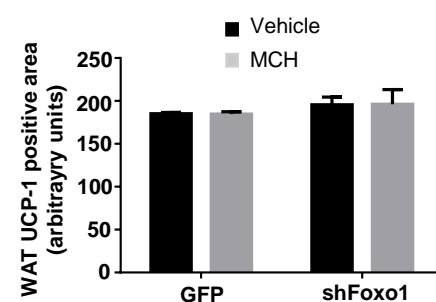
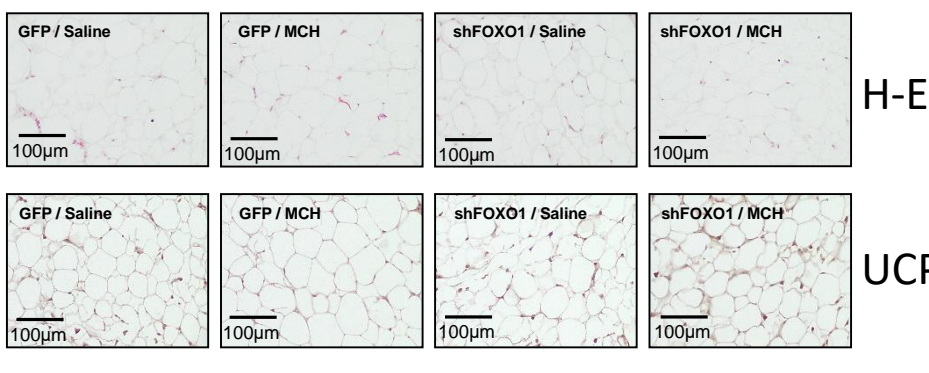
Figure S3



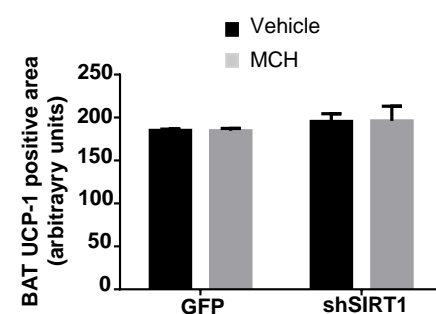
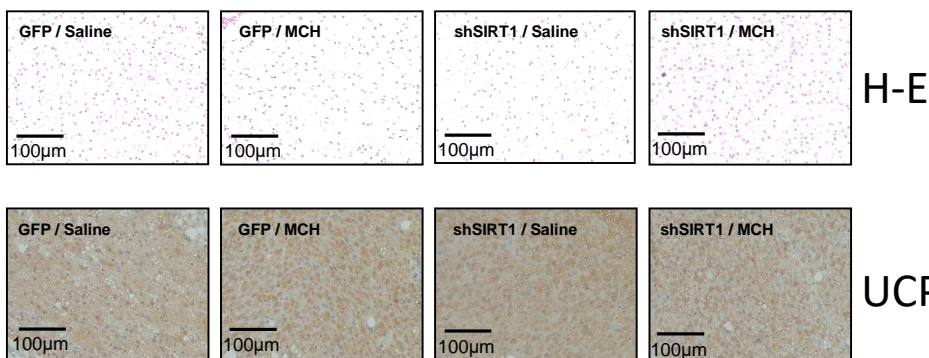
WAT shSIRT1



WAT shFOXO1



BAT shSIRT1



BAT shFOXO1

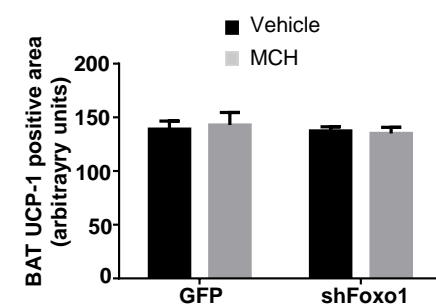
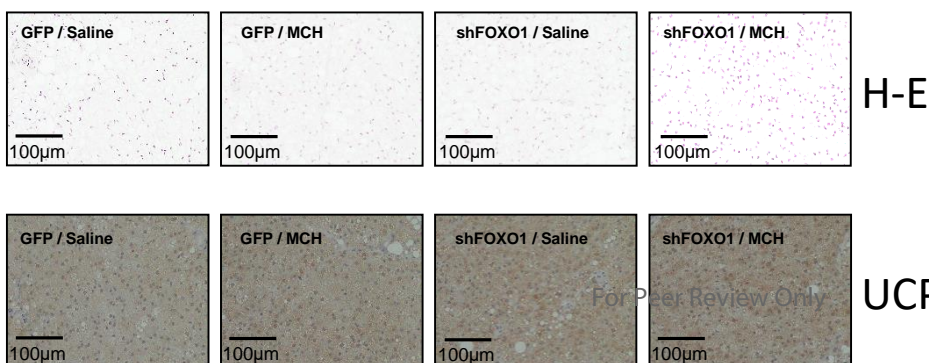
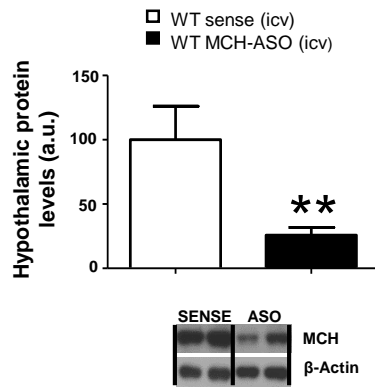
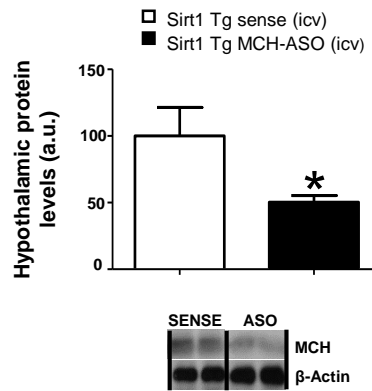


Figure S5

A



B



Supplementary information

Drugs

Rats received an intracerebroventricular (ICV) administration of 5 μ L of vehicle or MCH (20 μ g; Bachem, Bubendorf, Switzerland). For the inhibition of SIRT1, we used a potent specific inhibitor of SIRT1: Ex527 (10 μ g in a total volume of 5 μ L; Tocris Bioscience, St. Louis, MO). Mice were treated icv with MCH sense or MCH-ASO phosphorothioate-modified oligonucleotides. MCH sense and MCH-ASO were diluted in TE buffer (10 mM Tris-HCl, 1 mM EDTA) and injected at the beginning of the light cycle in a total volume of 2 μ l per mouse. Phosphorothioate modified oligonucleotides for MCH (sense, 5'-CCC TCA GTC TGG CTG-3' and anti-sense, 5'-ACA GCC AGA CTG AGG- 3') were obtained from Eurofins Genomix Company (Ebersberg, Germany) (1).

Stereotaxic microinjection of lentiviral expression vectors

Lentiviral vectors expressing green fluorescent protein (GFP) and inhibiting SIRT1 (shSIRT1), FOXO1 (shFOXO1), MCHR1 (shMCHR1), POMC (shPOMC) ($3,1 \times 10^6$ PFU/ml) (SIGMA-Aldrich) and GABA-R (shGABA-R) genes or scrambled sequences were injected bilaterally into the ARC (anterior to bregma (AP) -2.85 mm, lateral to the sagittal suture (L) $\pm 0,3$ mm, and ventral from the surface of the skull (V) -10,2 mm), with a microliter syringe (2; 3). The viral particles (1 μ l, $3,1 \times 10^6$ PFU/ml) were infused over 5 minutes and the injector kept in place for an additional 5 minutes. GFP fluorescence using a fluorescent visualized under the microscope was used as a visual marker of effective transduction of the lentivirus at the injection site. Dissection of the ARC was performed by micropunches under the microscope, as previously shown (4; 5).

Stereotaxic AAV-DREADD-mCherry injections

The hM3Dq coding sequences were cloned into a mCherry vector upstream of the mCherry sequence to generate C-terminal mCherry fusion proteins (Addgene, Cambridge, USA). The hM3Dq-mCherry coding sequence was amplified by PCR, and the amplicons and a cre-inducible AAV vector with a human *Synapsin 1* promoter was packaged in serotype 8: 7.53×10^{12} PFU/ml genome copies per mL and was prepared and tittered at the Universidad Autonoma de Barcelona (Barcelona, Spain). ketamine-xylazine anesthetized male *AgRP-Ires-cre* mice (6) were placed in a stereotaxic frame (David Kopf Instruments). The CRE-dependent AAV were injected bilaterally into the ARC of all mice (anterior to bregma (AP) -1.5 mm, lateral to the sagittal suture (L) ± 0.2 mm, and ventral from the surface of the skull (V) -6 mm) with a microliter syringe (neuros model 7001 KH, Hamilton, USA). The viral particles ($1 \mu\text{l}$, 7.53×10^9 PFU/ml) were infused over 10 minutes and the injector kept in place for an additional 5 minutes. Detection of mCherry was performed with an immunofluorescence procedure, using a rabbit anti-cherry (1:200; *Abcam*; Cambridge, UK). Detection was done with an anti-rabbit antibody conjugated with *Alexa 488* (1:200; *Molecular Probes*; Grand Island, NY, US)

Food intake experiments involving MCH-ASO or MCH-sense in *AgRP-Ires-cre* mice started after 30 min of CNO (1 mg/kg of body weight) or vehicle- i.p. injection. These mice were singly housed for at least 2 weeks beforehand.

Intracerebroventricular infusions

Rats and mice were anesthetized and cannulated to an osmotic minipump (model 2001 Alzet Osmotic Pumps; DURECT, CA) as previously described (2; 7). The minipump was inserted in subcutaneous pocket on the dorsal surface. MCH was continuously infused in rats and mice at the following concentrations: 10 µg/day and 2.5 µg/day respectively. The incision was closed with sutures, and rats were kept warm until full recovery.

Brain slice preparation

Hypothalamic slices were cut from 8- to 12-week-old male Pomc-Cre:ROSA-tdTomato mice as previously described (8). Briefly, mice were anaesthetized with isoflurane, and after decapitation, the brain was rapidly removed and put in ice-cold oxygenated (O₂ 95% / CO₂ 5%) artificial cerebrospinal fluid (ACSF) containing the following (in mM): 120 NaCl, 3.2 KCl, 1 NaH₂PO₄, 26 NaHCO₃, 1 MgCl₂, 2 CaCl₂, 2.5 glucose (osmolarity adjusted to 300 mOsm with sucrose, pH 7.4). After removal of the cerebellum, the brain was glued and coronal hypothalamic slices (250 µm thick) containing the ARC were cut using a vibratome (VT1200S; Leica). Before recording, slices were incubated at 35°C for a recovery period of 1 h. After recovery, slices were placed in a submerged recording chamber (31°C; Warner Instruments) and continuously perfused (2 ml/min) with oxygenated ACSF. Physiological concentration of glucose (2.5 mM) was used for recording (8). MCH was applied to the perfusing system (bath application) to obtain a final concentration of 1 µM.

Patch-clamp recordings

ARC POMC neurons expressing the fluorophore td-Tomato were visualized with a 40x objective in an upright video-microscope Leica DM-LFSA equipped with fluorescence

and infrared differential interference contrast (IR-DIC). Whole-cell patch-clamp recordings were performed in current-clamp mode as previously described (8) by using a Multiclamp 700B amplifier (Molecular Devices). Data were filtered at 1 kHz and sampled at 5 kHz with Digidata 1322A interface and Clampex 10.6 from pClamp software (Molecular Devices). Pipettes (from borosilicate capillaries; World Precision Instruments) had a resistance of 6-8 M Ω when filled with an internal solution containing the following (in mM): 123 K-gluconate, 2 MgCl₂, 8 KCl, 0.2 EGTA, 4 Na₂-ATP, 0.3 Na-GTP, and 10 HEPES, pH 7.3 with KOH. Loose patch-clamp recordings were performed in current-clamp mode. All recordings were analyzed with Clampfit 10.6 from pClamp software (Molecular Devices). Junction potential was determined to allow correction of membrane potential values. A series of current pulses from – 60 to 70 pA (1 s, 10 pA increments) was applied to measure the passive membrane properties of ARC POMC neurons.

Mean firing rate values were obtained before, during, and after MCH treatment. Neurons were considered responsive when a change of more than 20% in firing rate was observed. The peak response was determined, and the number of spikes was counted 2 min before and after the peak effect. Basal and recovery firing rate values were obtained by counting the number of spikes during a 4-min period before and after treatment, respectively.

Glucose tolerance test

Glucose-tolerance tests (GTT) were performed by injection of glucose (2 mg/g) intraperitoneally (ip) after 6 h fasting. Blood samples were collected immediately before and 15, 30, 60 and 120 min after glucose administration (9; 10).

Sympathetic nerve activity (SNA) recording

Mice were anesthetized with ip ketamine (91 mg kg⁻¹) and xylazine (9.1 mg kg⁻¹). Anesthesia was maintained with α -chloralose (initial dose: 25mg kg⁻¹, sustain dose: 50 mg kg⁻¹ h⁻¹) via a catheter inserted in the femoral vein. The trachea was cannulated, and each mouse was allowed to breathe spontaneously oxygen-enriched air. Rectal temperature was maintained at 37.5°C using a temperature-controlled surgical table and a lamp. We obtained multi-fiber recording of SNA as previously described (2). Using a dissecting microscope, a nerve fiber innervating WAT was identified, placed on the bipolar platinum-iridium electrode. Each electrode was attached to a high-impedance probe (HIP-511, Grass Instruments) and the nerve signal was amplified 105 times with a Grass P5 AC pre-amplifier. After amplification, the nerve signal was filtered at a 100- and 1000-Hz cutoff with a nerve traffic analysis system (Model 706C, University of Iowa Bioengineering). The nerve signal was then routed to an oscilloscope (model 54501A, Hewlett-Packard) for monitoring the quality of the sympathetic nerve recording and to a resetting voltage integrator (model B600c, University of Iowa Bioengineering). SNA measurements were made every 15 min for 6 h after icv. To ensure that electrical noise was excluded in the assessment of sympathetic outflow, we corrected each SNA recording for post-mortem background activity.

Western blot analysis

Western blot were performed as previously described (2; 11-13). Hypothalami, ARC, MBH, WAT and liver protein lysates were homogenized in ice-cold lysis buffer containing 50 mmol/L Tris-HCl (pH 7.5), 1 mmol/L EGTA, 1 mmol/l EDTA, 1% Triton X-100, 1 mmol/l sodium orthovanadate, 50 mmol/l sodium fluoride, 5 mmol/l sodium pyrophosphate, 0.27 mol/l sucrose, 0.1% 2-mercaptoethanol, and complete protease and

phosphatase inhibitor cocktail (1 tablet/50 ml; Roche Diagnostics, Mannheim, Germany). Homogenates were centrifuged at 13.000g for 10 min at 4°C, supernatants were removed, and aliquots were snap-frozen in liquid nitrogen. Hypothalamic and ARC protein lysates were subjected to SDS-PAGE on 8% and 12% polyacrylamide gels and electrotransferred on a polyvinylidene fluoride membrane. Briefly, total protein lysates from hypothalamus (40 µg) or ARC (20 µg) were subjected to SDS-PAGE, electrotransferred on a polyvinylidene difluoride membrane. Membranes were blocked for 1 h in TBS-Tween 20 (TBST: 50 mmol/L Tris- HCl (pH 7.5), 0.15 mol/L NaCl, and 0.1% Tween 20) containing 5% skimmed milk or 3% BSA and probed for 16 h at 4°C in TBST, 5% skimmed milk or 3% BSA with antibodies against ACC, phospho-ACC-Ser79 (pACC), AMPK α 1 and AMPK α 2 (Upstate); phospho-AMPK-Thr172 (pAMPK), pHSL Ser680, SAPK/JUNK Thr183/Tyr185, FOXO1, acetyl-p53 and p53 (Cell Signaling); AgRP (Abcam); POMC, NPY, CART, FAS(H-300), SIRT1, CIDE-A (N-19)R, acetyl-Foxo1, GABA-R and MCH pro-peptide (Santa Cruz Biotechnology), MCHR1 (Abnova) or mTOR, p-mTOR and β -actin (Sigma-Aldrich). Given that some processed peptides are short and are unlikely to be electrophoretically resolved in a blot of polyacrylamide gel we used antibodies detecting pre-propeptides for POMC, NPY and AgRP (for more information please see supplementary **Table S2**). Because some mature peptides are too short to be electrophoretically resolved in a blot of polyacrylamide gel, we used antibodies detecting pre-propeptides for POMC, NPY and AgRP (for more information please see supplementary **Table S2**). Membranes were then incubated with horseradish peroxidase-conjugated secondary antibodies (Dako Denmark, Glostrup, Denmark) followed by chemiluminescence (Pierce ECL Western Blotting Substrate, Thermo scientific, USA). Then, the membranes were exposed to X-ray film (Super RX, Fuji Medical X-Ray Film, Fujifilm, Japan) and developed with developer and fixing liquids (AGFA, Germany)

under appropriate dark room conditions. Protein levels were normalized to β -actin for each sample.

Real-time PCR

Real-time PCR (*TaqMan*®, *Applied Biosystems*; Foster City, CA, USA; or *SYBR*® *Green*, *Roche Molecular Biochemicals*, Mannheim, Germany, for the hypothalamic nuclei samples) was performed using specific primers and probes (**Table S1**) as previously described (14). Values were expressed in relation to hypoxanthineguanine phosphoribosyl-transferase (HPRT) levels.

Liver TG content

The extraction procedure for liver TG was adapted from methods described previously (2). Livers (approx 200 mg) were homogenized for 2 min in ice-cold chloroform-methanol (2:1, vol/vol). TG were extracted during 5-h shaking at room temperature. For phase separation, H₂O MQ was added, samples were centrifuged, and the organic bottom layer was collected. The organic solvent was dried using a Speed Vac and dissolved in chloroform. TG (Randox Laboratories LTD, UK) content of each sample was measured in duplicate after evaporation of the organic solvent using an enzymatic method.

Hematoxylin/eosin staining and immunohistochemistry

WAT and BAT samples were fixed in 10% formalin buffer for 24 h, and then dehydrated and embedded in paraffin by a standard procedure. Sections of 3 μ m were prepared with a microtome and stained using a standard Hematoxylin/Eosin Alcoholic (BioOptica) procedure according to the manufacturer's instructions. Alternative sections of paraffin were used for immunohistochemistry detection of UCP-1. Immunohistochemistry was

performed as previously described (15; 16) using a rabbit anti-UCP-1 (1:500 for WAT and 1:2000 for BAT; Abcam; Cambridge, UK). UCP-1-positive cells were counted by using Image J.

Immunofluorescence

Mice brains were fixed by perfusion followed by immersion (12 h) in 10% buffered formalin for 24 hours. The brain pieces were cut 50 μ m thick using a Vibratome® Series 1000. Detection of GFP, and POMC immunofluorescence; and double labelling were performed as previously reported (15; 17).

Supplementary figure legends

Supplementary Figure 1. Protein expression of some molecular markers after central MCH administration in the ARC. Central effects of icv MCH administration (20µg/rat) on, **(A)** hypothalamic protein levels of FAS, ACC, pACC, AMPKα1, AMPKα2, pAMPK, mTOR and p-mTOR and **(B)** hypothalamic protein levels of NPY and CART in rats after 2 hours. β-actin was used to normalize protein levels. Dividing lines indicate spliced bands from the same gel. Values are mean ± SEM of 7–10 animals per group.

Supplementary Figure 2. Intracellular pathway induced by MCH in the ARC and specificity of the nuclei isolation. mRNA levels of FOXO1 (A), POMC (B) and AgRP (C) in the ARC after icv injection of MCH. VMH FOXO1 mRNA (D) and LHA (E) FOXO1 mRNA expression after icv MCH injection. VMH SIRT1 and FOXO1 protein levels (F) and LHA SIRT1 and FOXO1 protein levels (G) after the injection of MCH directly in the ARC. mRNA levels of POMC (H) and SF-1 (I) were measured in the ARC and VMH. Values are mean ± SEM of 5–8 animals per group. * $P \leq 0.05$, ** $P \leq 0.01$ and *** $P \leq 0.001$ vs controls.

Supplementary Figure 3. The MCH orexigenic action is blunted by the pharmacological blockade of SIRT1. Effects of icv injection of MCH (20µg/rat) and EX-527 (10µg/rat) + MCH (20µg/rat) compared to vehicle injected controls on food intake after 2h (A). Body weight change (B) and cumulative food intake (C) after 2 weeks of shSIRT1 injection or GFP scrambled lentiviruses into the ARC of rats before

MCH administration. Values are mean \pm SEM of 8–10 animals per group. * $P\leq 0.05$, ** $P\leq 0.01$; and *** $P\leq 0.001$ vs controls.

Supplementary Figure 4. Central MCH requires SIRT1 and FoxO1 in the hypothalamic ARC to induce adiposity. Representative pictures of WAT and BAT histology (hematoxylin-eosin) and WAT and BAT protein levels of UCP1; Values are mean \pm SEM of 5–10 animals per group.

Supplementary Figure 5. Central inhibition of MCH induces hypophagia. MCH protein levels in the different models evaluated with MCH-ASO: wild type mice (A) and SIRT1 Tg mice (B). Values are mean \pm SEM of 5–10 animals per group. * $P\leq 0.05$, ** $P\leq 0.01$; and *** $P\leq 0.001$ vs controls.

Appendix figures. Uncropped blots.

mRNA	Gene name	Gene bank accession number	Sequence of primers
AgRP	Agouti-related protein	NM 00360.1	FWD: 5'-CAG AGT TCT CAG GTC TAA GTC-3' REV: 5'-TTG AAG AAG CGG CAG TAG CAC-3'
FoxO1	Forkhead box protein O1	NM 001191846.2	FWD: 5'-TGT GCC CTA CTT CAA GGA TAA GG-3' REV: 5'-GTG GCG AAT TGA ATT CTT CCA-3'
Hprt	Hypoxanthine Phosphoribosyltransferase-1	NM 012583	FWD: 5'-AGC CGA CCG GTT CTG TCA T-3' REV: 5'-GGT CAT AAC CTG GTT CAT CAT CAC-3'
POMC	Pro-opiomelanocortin	NM 139326.2	FWD: 5'-CGT CCT CAG AGA GCT GCC TTT-3' REV: 5'-TGT AGC AGA ATC TCG GCA TCT TC-3'
Sf-1	Steroidogenic factor-1		Assay ID Applied Biosystems TaqMan® Gene Expression Assays Assay ID Rn00584298_m1

Supplementary Table 1 related to Figure S2: Primers and probes for real-time PCR (TaqMan®) analysis.

Protein	Name of Antibody	Manufacturer, catalog and lot #, and/or name of individual providing the antibody	Species raised in	Dilution used	Lot
ACC	Anti-ACC	Millipore, 04-322	rabbit	1:1000	Not available
Acetyl Foxo1	Anti-Acetyl-FKHR	Santa Cruz Biotechnology, sc-101681	rabbit	1:1000	DO915
Acetyl-p53	Anti-acetyl p53	Cell Signaling, #2570	rabbit	1:500	4
AgRP	Anti-AgRP propeptide	Abcam, ab113481	rabbit	1:1000	GR66371-6
AMPKα1	Anti-AMPK α 1	Millipore #07-350	rabbit	1:1000	2684946
AMPKα2	Anti-AMPK α 2	Millipore #07-363	rabbit	1:1000	2475668
β-actin	Anti- β -Actin	Sigma-Aldrich A 5316	mouse	1:10000	067M4781V
CART	Anti-CART (N20)	Santa Cruz Biotechnology, sc-18068	GOAT	1:1000	I1911
CIDE-A	Anti-CIDE-A (N-19)R	Santa Cruz Biotechnology, sc-8730-R	rabbit	1:1000	K1209
FAS	Anti-FAS (H-300)	Santa Cruz Biotechnology, sc-20140	rabbit	1:1000	G1813
FOXO1	Anti-Fox01 (C29H4)	Cell Signaling, #2880	rabbit	1:1000	11
GABA-R	Anti-GABA-RAP (FL-117)	Santa Cruz Biotechnology sc-28938	rabbit	1:1000	J2708
GFP	Anti-GFP	Abcam, ab13970	chicken	1:4000	GR3190550-14
MCH	Anti-MCH pro-peptide	Santa Cruz Biotechnology sc-28931	rabbit	1:1000	B2006
MCHR1	Anti-MCH-R	Abnova PAB16225	rabbit	1:1000	5487/5488AP3-1
mTOR	Anti-mTOR	Cell Signaling, #2972	rabbit	1:1000	10
NPY	Anti-NPY propeptide	Sigma-Aldrich, WH0004852	mouse	1:1000	09121-3B5
pACC	Anti-phospho-ACC-Ser79	Cell Signaling, #3661	rabbit	1:1000	10
pAMPK	Anti-phospho-AMPK-Thr172	Cell Signaling, 2535	rabbit	1:1000	21
pHSL	Anti-phospho HSL (ser 680)	Cell Signaling, 4126	rabbit	1:1000	6
pJNK	Anti-SAPK/JUNK Thr183/Tyr185	Cell Signaling, #4668	rabbit	1:1000	11
p-mTOR	Anti-p-mTOR (Ser 2448)	Cell Signaling, #2971	rabbit	1:1000	21
POMC	Anti-POMC propeptide (FL-267)	Santa Cruz Biotechnology, sc-20148	rabbit	1:1000	G2810
POMC	Anti-POMC propeptide	Phoenix pharmaceuticals, H029-30	rabbit	1:200	01800-4
p53	Anti-p53 (1C12) mouse mAB	Cell Signaling, #2524S	mouse	1:1000	13
SIRT1	Anti-SIRT1 (H-300)	Santa Cruz Biotechnology, sc-15404	rabbit	1:1000	Not available

Supplementary Table 2: List of antibodies used in the western blots and immunohistochemistry methods.

Supplementary references

1. Pereira-da-Silva M, De Souza CT, Gasparetti AL, Saad MJ, Velloso LA: Melanin-concentrating hormone induces insulin resistance through a mechanism independent of body weight gain. *J Endocrinol* 2005;186:193-201
2. Imbernon M, Beiroa D, Vazquez MJ, Morgan DA, Veyrat-Durebex C, Porteiro B, Diaz-Arteaga A, Senra A, Busquets S, Velasquez DA, Al-Massadi O, Varela L, Gandara M, Lopez-Soriano FJ, Gallego R, Seoane LM, Argiles JM, Lopez M, Davis RJ, Sabio G, Rohner-Jeanrenaud F, Rahmouni K, Dieguez C, Nogueiras R: Central melanin-concentrating hormone influences liver and adipose metabolism via specific hypothalamic nuclei and efferent autonomic/JNK1 pathways. *Gastroenterology* 2013;144:636-649 e636
3. Aponte Y, Atasoy D, Sternson SM: AGRP neurons are sufficient to orchestrate feeding behavior rapidly and without training. *Nature neuroscience* 2011;14:351-355
4. Martinez de Morentin PB, Gonzalez-Garcia I, Martins L, Lage R, Fernandez-Mallo D, Martinez-Sanchez N, Ruiz-Pino F, Liu J, Morgan DA, Pinilla L, Gallego R, Saha AK, Kalsbeek A, Fliers E, Bisschop PH, Dieguez C, Nogueiras R, Rahmouni K, Tena-Sempere M, Lopez M: Estradiol regulates brown adipose tissue thermogenesis via hypothalamic AMPK. *Cell Metab* 2014;20:41-53
5. Imbernon M, Sanchez-Rebordelo E, Gallego R, Gandara M, Lear P, Lopez M, Dieguez C, Nogueiras R: Hypothalamic KLF4 mediates leptin's effects on food intake via AgRP. *Mol Metab* 2014;3:441-451
6. Koch M, Varela L, Kim JG, Kim JD, Hernandez-Nuno F, Simonds SE, Castorena CM, Vianna CR, Elmquist JK, Morozov YM, Rakic P, Bechmann I, Cowley MA, Szigeti-Buck K, Dietrich MO, Gao XB, Diano S, Horvath TL: Hypothalamic POMC neurons promote cannabinoid-induced feeding. *Nature* 2015;519:45-50
7. Gomori A, Ishihara A, Ito M, Mashiko S, Matsushita H, Yumoto M, Tanaka T, Tokita S, Moriya M, Iwaasa H, Kanatani A: Chronic intracerebroventricular infusion of MCH causes obesity in mice. Melanin-concentrating hormone. *Am J Physiol Endocrinol Metab* 2003;284:E583-588
8. Clasadonte J, Scemes E, Wang Z, Boison D, Haydon PG: Connexin 43-Mediated Astroglial Metabolic Networks Contribute to the Regulation of the Sleep-Wake Cycle. *Neuron* 2017;95:1365-1380 e1365
9. Perez-Sieira S, Martinez G, Porteiro B, Lopez M, Vidal A, Nogueiras R, Dieguez C: Female Nur77-deficient mice show increased susceptibility to diet-induced obesity. *PLoS one* 2013;8:e53836
10. Contreras C, Gonzalez-Garcia I, Martinez-Sanchez N, Seoane-Collazo P, Jacas J, Morgan DA, Serra D, Gallego R, Gonzalez F, Casals N, Nogueiras R, Rahmouni K, Dieguez C, Lopez M: Central ceramide-induced hypothalamic lipotoxicity and ER stress regulate energy balance. *Cell reports* 2014;9:366-377
11. Beiroa D, Imbernon M, Gallego R, Senra A, Herranz D, Villarroya F, Serrano M, Ferno J, Salvador J, Escalada J, Dieguez C, Lopez M, Fruhbeck G, Nogueiras R: GLP-1 Agonism Stimulates Brown Adipose Tissue Thermogenesis and Browning Through Hypothalamic AMPK. *Diabetes* 2014;63:3346-3358
12. Lopez M, Lage R, Saha AK, Perez-Tilve D, Vazquez MJ, Varela L, Sangiao-Alvarellos S, Tovar S, Raghay K, Rodriguez-Cuenca S, Deoliveira RM, Castaneda T, Datta R, Dong JZ, Culler M, Sleeman MW, Alvarez CV, Gallego R, Lelliott CJ, Carling D, Tschop MH, Dieguez C, Vidal-Puig A: Hypothalamic fatty acid metabolism mediates the orexigenic action of ghrelin. *Cell Metab* 2008;7:389-399
13. Lopez M, Varela L, Vazquez MJ, Rodriguez-Cuenca S, Gonzalez CR, Velagapudi VR, Morgan DA, Schoenmakers E, Agassandian K, Lage R, Martinez de Morentin PB, Tovar S, Nogueiras R, Carling D, Lelliott C, Gallego R, Oresic M, Chatterjee K, Saha AK, Rahmouni K, Dieguez C, Vidal-Puig A: Hypothalamic AMPK and fatty acid metabolism mediate thyroid regulation of energy balance. *Nature medicine* 2010;16:1001-1008

14. Zhan C, Zhou J, Feng Q, Zhang JE, Lin S, Bao J, Wu P, Luo M: Acute and long-term suppression of feeding behavior by POMC neurons in the brainstem and hypothalamus, respectively. *The Journal of neuroscience : the official journal of the Society for Neuroscience* 2013;33:3624-3632
15. Quinones M, Al-Massadi O, Folgueira C, Bremser S, Gallego R, Torres-Leal L, Haddad-Tovoli R, Garcia-Caceres C, Hernandez-Bautista R, Lam BYH, Beiroa D, Sanchez-Rebordelo E, Senra A, Malagon JA, Valerio P, Fondevila MF, Ferno J, Malagon MM, Contreras R, Pfluger P, Bruning JC, Yeo G, Tschop M, Dieguez C, Lopez M, Claret M, Kloppenburg P, Sabio G, Nogueiras R: p53 in AgRP neurons is required for protection against diet-induced obesity via JNK1. *Nat Commun* 2018;9:3432
16. Al-Massadi O, Porteiro B, Kuhlow D, Kohler M, Gonzalez-Rellan MJ, Garcia-Lavandeira M, Diaz-Rodriguez E, Quinones M, Senra A, Alvarez CV, Lopez M, Dieguez C, Schulz TJ, Nogueiras R: Pharmacological and Genetic Manipulation of p53 in Brown Fat at Adult But Not Embryonic Stages Regulates Thermogenesis and Body Weight in Male Mice. *Endocrinology* 2016;157:2735-2749
17. Quinones M, Al-Massadi O, Gallego R, Ferno J, Dieguez C, Lopez M, Nogueiras R: Hypothalamic CaMKKbeta mediates glucagon anorectic effect and its diet-induced resistance. *Mol Metab* 2015;4:961-970